# 内蒙古北山石板井地区晚古生代中酸性侵入杂岩 LA-ICP-MS 年龄和地球化学特征及其地质意义

赵克强,马生明,席明杰,杨剑洲,蔡永文,龚晶晶
中国地质科学院地球物理地球化学勘查研究所,河北廊坊,065000

**内容提要**:花岗岩的时代和地球化学特征可以揭示岩浆源、形成环境和构造演化。近期我们在从事内蒙古黑鹰山地区矿产地质调查和相关科研工作过程中,在石板井地区发现一套中泥盆世中酸性侵入杂岩,为了揭示它们的岩浆源、形成环境和构造演化,我们在野外地质调查研究的基础上,开展了锆石 U-Pb 定年、岩石元素地球化学的系统测定。研究表明:细粒辉石闪长岩—中粒花岗闪长岩—中细粒花岗闪长岩—中粒黑云母二长花岗岩形成时代为中泥盆世(385~380 Ma),具有同源岩浆演化特征。其中,细粒辉石闪长岩具有钙碱性、钠质、准铝质岩石属性;中粒黑云母二长花岗岩—中粒花岗闪长岩—中细粒花岗闪长岩具有高钾钙碱性—钙碱性、钾质—钠质、过铝质—准铝质岩石属性;初始岩浆可能是俯冲板片流体交代的地幔楔,地幔楔部分熔融形成玄武质岩浆,玄武质岩浆底侵而导致上覆年轻地壳的部分熔融的产物,在此过程中伴随着分离结晶作用;中泥盆世中酸性侵入杂岩具有 I 型花岗岩的特征,其形成于大洋岛弧背景下的火山弧环境,可能是小黄山洋向南俯冲的产物。

**关键词**:中酸性侵入杂岩;元素地球化学;中泥盆世;锆石 U-Pb 定年;内蒙古北山石板井地区

北山地区是中亚造山带的重要组成部分(Jahn et al., 2004;Xiao Wenjiao et al.,2010),也是我国重要的铜、铅、锌、铁、金、钒钛磁铁矿多金属成矿带,到目前为止已发现了矽卡岩型 Cu、Fe、Pb 矿床(辉铜山铜矿床、花牛山铅锌矿床)、斑岩型 Cu、Mo 矿床(公婆泉铜矿床、三道明水铜金矿床、白山堂铜矿床)、火山岩型 Fe、Au 矿床(黑鹰山铁矿床、老金厂金矿床、马庄山金矿床和新金厂金矿床)、以及与镁铁质岩有关 V—Ti—Fe 矿床(小红山钒钛磁铁矿矿床)等在内的一批贵金属、有色金属及黑色金属矿床,这些矿床的形成与区内构造—岩浆活动关系密切(聂凤军等,2000;Jiang Sihong et al., 2004, 2005)。独特的构造位置、复杂而强烈的构造—岩浆活动,种类繁多的矿产资源,使得北山地区逐渐受到地质工作者的广泛关注(左国朝等,1990;聂凤军等,2000,2002,2003;江思宏等,2003;孙新春等,2011;Song Dongfang et al.,2013,2014;王国强等,2016;Ding Jiaxin et al.,2017;陈超等,2017;赵振明等,2018;许伟等,2019)。北山地区由南向北分布着柳园—音凹峡、红柳河—牛圈子—洗肠井、明水—石板井—小黄山、红石山—百合山—蓬勃山等四条重要蛇绿岩带(左国朝等,1990;杨和群等,2010;Su Benxun et al.,2012;Liu Qian et al.,2015)。前人通过北山地区岩浆岩的研究,已初步建立了区域年代学格架;北山构造带岩浆作用主要为花岗岩浆作用(聂凤军等,2002),大致可划分出前寒武纪、早古生代、晚古生代和中生代四期。其中,古生代花岗岩浆活动在该区最为强烈;这使得人们对该区岩浆及其构造演化有了进一步的认识(王立社等,2009;Li Shan et al.,2013;Song Dongfang et al.,2015;郑国荣等,2016;赵志雄等, 2018;Wang Xinyu et al.,2018;赵宏刚等,2019),但对于位于塔里木板块和西伯利亚板块之间的晚古生代侵入岩的成因及其构造演化研究较少(刘亚雪等,1995;江思宏等,2006;李舢等,2009,2011)。本文对北山石板井地区中泥盆世中酸性侵入杂岩进行了野外地质调查、年代学、地球化学等方面的研究,以揭示该区中酸性侵入杂岩的形成时代、地球化学特征、岩浆的源区性质及其构造背景;为深入揭示北山地区晚古生代岩浆演化和构造背景提供科学依据。

## 1 地质概况及岩体特征

注:本文为中国地质调查局地质调查项目(编号:DD20160040、DD20190570、DD20190571)的成果。
收稿日期:2019-04-14;改回日期:2019-08-18;责任编辑:章雨旭。Doi:10.16509/j.georeview.2020.01.005
作者简介:赵克强,男,1986年生,博士研究生,矿物学、岩石学、矿床学专业,Email:zhaokeqiang@igge.cn。

### 1.1 地质概况

北山造山带位于中亚造山带南缘,处于西伯利亚板块、塔里木板块和华北板块的交汇部位,南邻敦煌地块,北接蒙古增生造山带(Xiao Wenjiao et al., 2010)(图 1a),区域上发育的地层以元古宙变质—火山—沉积岩群、古生代海相火山岩与碎屑岩和新生代碎屑岩为主,以及少量的中生代陆相火山—碎屑岩地层;本区构造非常复杂,整体上,北山从南至北被 4 条蛇绿岩带分割,依次发育石板山—双鹰山——→花牛山—马鬃山—公婆泉——→月牙山—黑鹰山——→旱山—雀儿山地体;发育一系列近东西向的北凸弧形大断裂分割的断块系统,局部呈 NWW 向,同时发育 NW、NE 和 NNE 向次级断裂;此外,古老断块之上发育盖层,盖层中发育褶曲,形成一些复式背斜,其后又被长轴北东向的中—新生代断陷盆地所分割。区域上侵入岩分布广泛,以古生代为主,主要以岩基或岩株状产出,少数以岩脉状产出(邓自华,1965;刘雪亚,1984;左国朝等,1990;刘雪亚等,1995)。

研究区位于北山造山带中段,东部接壤于阿拉善,西部毗邻东天山,位于石板墩和星星峡两大走滑断裂之间,属公婆泉—月牙山地体(左国朝等,1990)。其南北两侧分别受明水—石板井—小黄山和红柳河—牛圈子—洗肠井蛇绿岩带控制,呈狭长的东西向带状分布(刘雪亚等,1995)(图 1b),区内地层主要为元古宙变质—沉积岩群和中生代陆相碎屑岩为主,同时含有少量的古生代变质火山岩和新生代地层;构造线以北西向为主;侵入岩主要为晚志留世花岗岩和中泥盆世花岗质岩石。

### 1.2 石板井地区中泥盆世侵入杂岩的地质、岩相学特征

研究区泥盆纪侵入岩主要由花岗闪长岩、二长花岗岩和辉石闪长岩组成,以及与花岗岩相伴生的岩脉等。其中花岗闪长岩为研究区泥盆纪侵入岩的主体岩性,主体岩石以块状构造为主,局部花岗岩内含有暗色包体(图 3a);本次研究共采集了 21 件样品,岩性为花岗闪长岩、二长花岗岩和辉石闪长岩,采样位置(图 2)。4 件用于挑选锆石进行 LA-ICP-MS 定年分析,17 件用于岩石地球化学测试,其中花岗闪长岩 8 件,二长花岗岩 6 件,辉石闪长岩 3 件。它们的岩相学特征分述如下:

花岗闪长岩:主要呈不规则岩基状产出,区内出

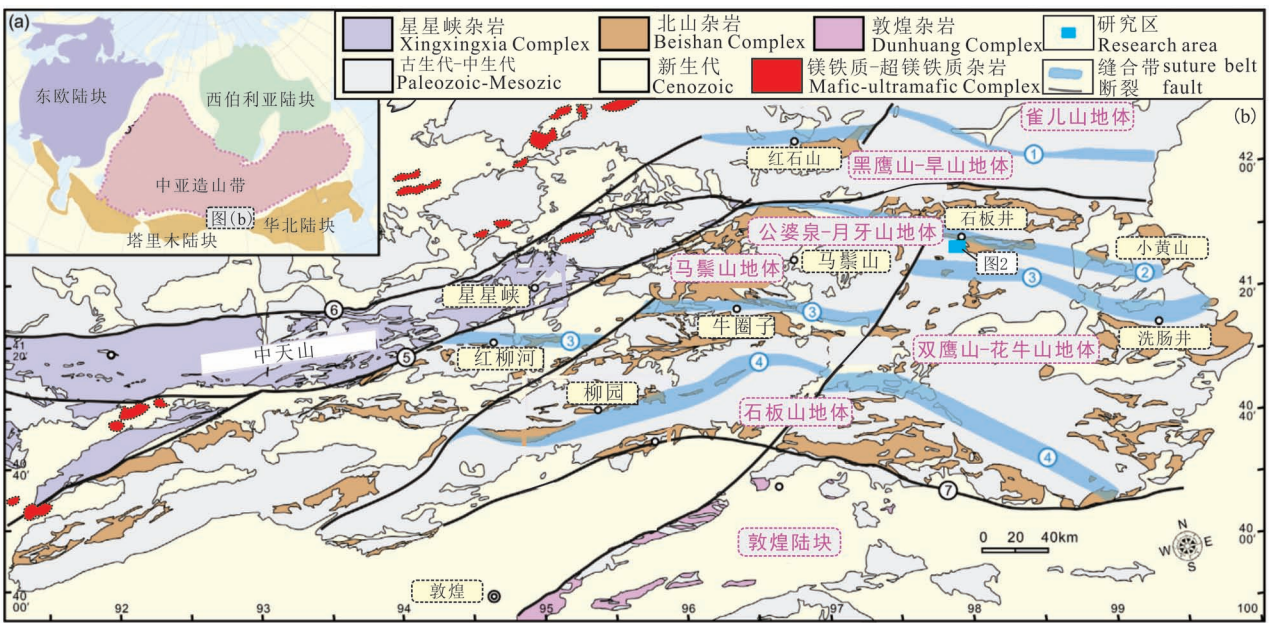


图 1(a)中亚造山带构造格架简图;(b)北山造山带构造简图(据 Su Benxun et al.,2012;Liu Qian et al.,2015 改)

Fig. 1 (a) Simplified tectonic sketch map of the Central Asian Orogenic Belt, (b) Geological sketch map of the Beishan Orogenic Belt(modified from Su Benxun et al., 2012; Liu Qian et al., 2015)

①红石山—百合山—蓬勃山蛇绿岩带;②明水—石板井—小黄山蛇绿岩带;③红柳河—牛圈子—洗肠井蛇绿岩带;④柳园—音凹峡蛇绿岩带;⑤星星峡断裂;⑥沙泉子断裂;⑦石板墩断裂

① Hongshishan—Baiheshan—Pengboshan mélange, ② Mingshui—Shibanjing—Xiaohuangshan mélange, ③ Hongliuhe—Niujuanzi—Xichangjing mélange, ④ Liuyuan—Yinaoxia mélange, ⑤ Xingxingxia fault, ⑥ Shaquanzi fault, ⑦ Shibandun fault

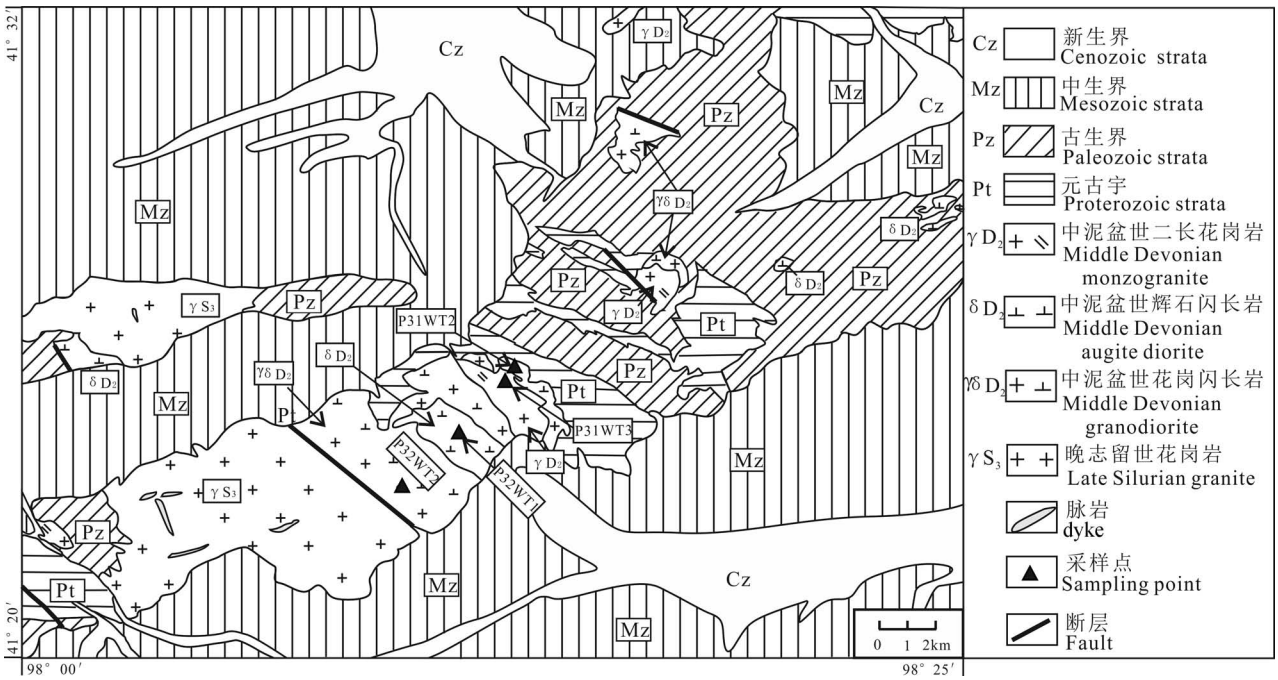


图 2 内蒙古北山石板井南部地区地质图

Fig. 2 Geological map of the southern part of the Shibanjing area, Beishan Mountains, Inner Mongolia

露面积 18.5 $km^2$,中细粒半自形结晶结构,块状构造;矿物组成:斜长石(40%~45%)+碱性长石(5%~10%)+石英(20%~25%)+普通角闪石(15%~20%)+黑云母(1%~2%)。其中,斜长石呈自形—半自形板柱状,发育聚片双晶,部分发生粘土化蚀变;角闪石呈柱状,发育菱形解理,局部发生绿泥石化和绿帘石化;副矿物主要为少量的榍石、锆石和磁铁矿(图 3b)。

二长花岗岩:分布于花岗闪长岩岩基内部,呈渐变岩株状产出,区内出露面积 4.5 $km^2$,中细粒自形、半自形粒状结晶结构、块状构造;矿物组成:碱性长石(30%~35%)+斜长石(25%~30%)+石英(35%~40%)+黑云母(3%~8%);其中,碱性长石呈半自形—它形板柱状,部分碱性长石发育格子双晶,为微斜长石;斜长石呈自形—半自形板柱状,发育聚片双晶,部分发生粘土化蚀变;石英呈半自形粒状,少数呈集合体状;其中,大的碱性长石内部可见条板状、个别浑圆条板状的小斜长石晶体及细小的片状黑云母(图 3c)。

辉石闪长岩:主要分布在花岗闪长岩岩基中,呈渐变岩株状产出,区内出露面积 3.8 $km^2$,细粒结构,块状构造。其斜长石含量(65%~70%)+角闪石含量(20%~25%)+辉石含量(5%~10%)(图 3d)。

## 2　分析方法

锆石的分选在河北省区域地质调查院实验室完成,阴极发光照相(CL)在配备阴极荧光探头的 JSM6510 型扫描电镜上完成;锆石 LA-ICP-MS 定年工作在中国地质科学院资源研究所完成,锆石定年分析所用仪器为 Finnigan Neptune 型 MC-ICP-MS 及与之配套的 Newwave UP 213 激光剥蚀系统。激光剥蚀斑束直径为 32 μm,频率为 10 Hz;LA-MC-ICP-MS 激光剥蚀采样采用单点剥蚀的方式,数据分析前用锆石 GJ-1 调试仪器,使之达到最优状态;以 GJ-1 位外标进行校正,测试过程中每 5~7 个样品前后重复测定 2 次锆石 GJ-1 对样品进行校正,元素含量采用 SRM 610 为外标;测试过程参考胡古月等(2015);数据处理采用 ICPMS DataCal 程序(Liu Yongsheng et al., 2008, 2010),锆石年龄谐和图用 Isoplot 3. 0 程序处理。具体原理和流程参考侯可军等(2009)。测试结果见表 1。

样品主量元素、微量元素、稀土元素测试工作在辽宁省地质矿产研究院实验室完成。其中主量元素采用 Axios MaxX-荧光光谱仪进行分析,Cs、Ba、Nb、Rb、Zr 元素用 X 荧光光谱法分析,V、Sn、Cr、Ni、Hf、Sr、Ta、Th、U 和 REE 等元素用电感耦合等离子体质

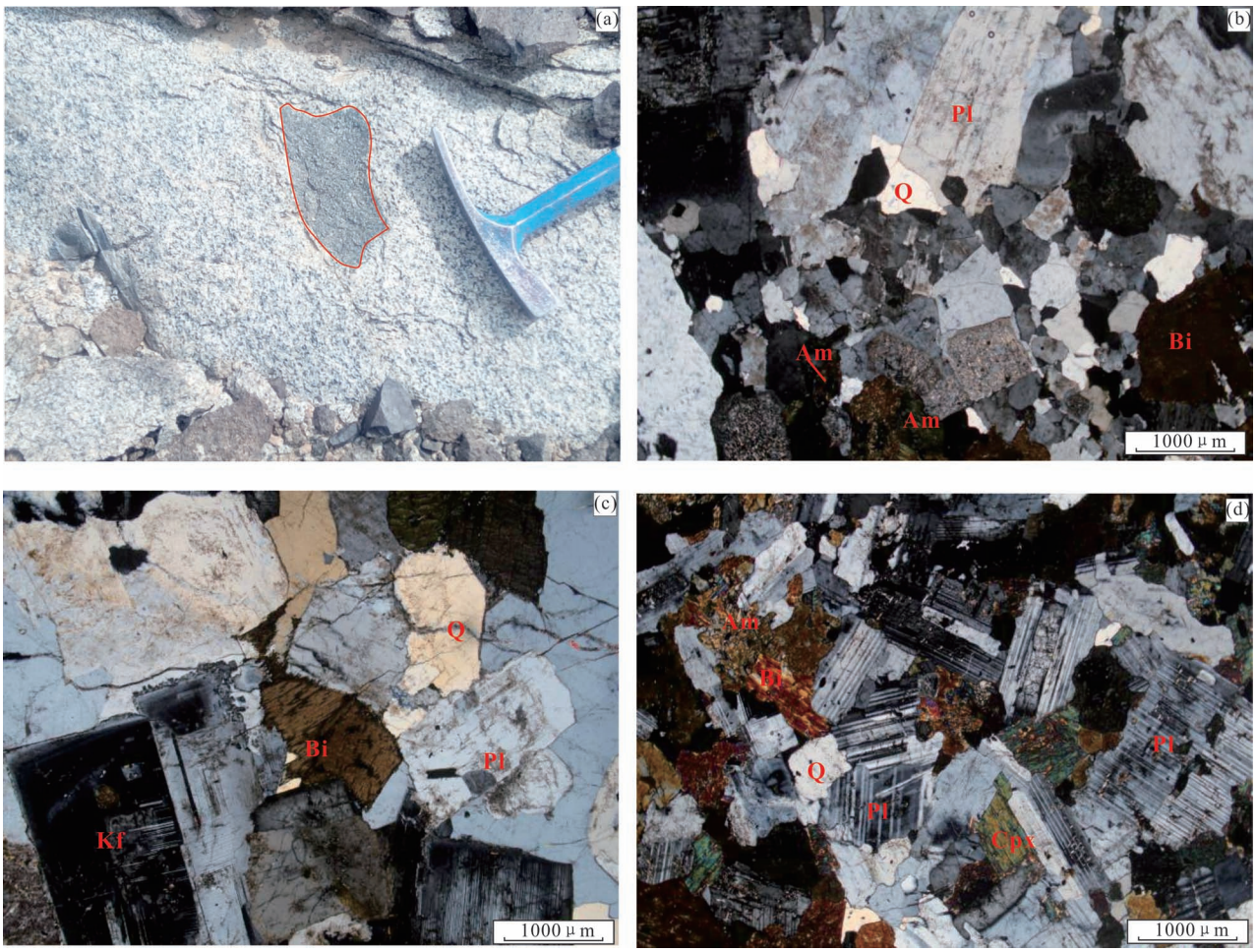


图 3 北山石板井地区侵入杂岩野外和偏光显微镜下照片

Fig. 3 Photograph and photomicrographs (in crossed polar) of the rocks for the granite in Shibanjing area, Beishan Mountains

Pl—斜长石；Kf—钾长石；Cpx—单斜辉石；Am—角闪石；Q—石英；Bi—黑云母

Pl—plagioclase)；Kf— feldspar；Cpx—clinopyroxene；Am—amphibole；Q—quartz；Bi—biotite

谱法(ICP-MS)分析,具体过程参考(Zhao Keqiang et al.,2017)。主微量元素分析结果见表 2。

## 3 分析结果

### 3.1 锆石 LA-ICP-MS 定年

中粒二长花岗岩(P31WT2)锆石粒径在 100~150 μm 之间,长宽比多数为 1.5∶1~2∶1,少数可达 2.5∶1。CL 图像显示(图 4a),内部振荡环带结构发育。对 19 粒锆石的分析结果表明,$n(^{206}Pb)/n(^{238}U)$表面年龄变化在 377~388 Ma(表 1,图 5b),其$n(^{206}Pb)/n(^{238}U)$加权平均年龄为 381.7±0.9 Ma($n$=19,MSWD=1.09,图 5a),表明二长花岗岩结晶年龄为 380 Ma 左右。

中细粒花岗闪长岩(P31WT3)锆石粒径一般在 100~180 μm,长宽比多数为 1.2∶1~2.5∶1。CL 图像显示(图 4b),多为自形—半自形晶,呈聚形双锥柱状,内部发育岩浆振荡环带结构。对 16 粒锆石的分析结果表明,单颗粒锆石 U—Pb 测年结果是:$n(^{206}Pb)/n(^{238}U)$表面年龄变化在 379~393 Ma(表 1,图 5d),其 $n(^{206}Pb)/n(^{238}U)$加权平均年龄为 386.3±1.0 Ma($n$=16,MSWD=7.3,图 5c),表明中细粒花岗闪长岩结晶年龄为 386 Ma 左右。

细粒辉石闪长岩(P32WT1)锆石粒径一般为 90~150 μm,长宽比多数为 1∶1~1.5∶1。CL 图像显示(图 4c),多为半自形晶呈聚形双锥柱状或浑圆状,内部环带结构发育。对 21 粒锆石的分析结果表明,$n(^{206}Pb)/n(^{238}U)$表面年龄变化在 381~389 Ma(表 1,图 5f),其 $n(^{206}Pb)/n(^{238}U)$加权平均年龄为 385.6±1.0 Ma($n$=21,MSWD=11,图 5e),表明细粒辉石闪长岩结晶年龄为 385 Ma 左右。

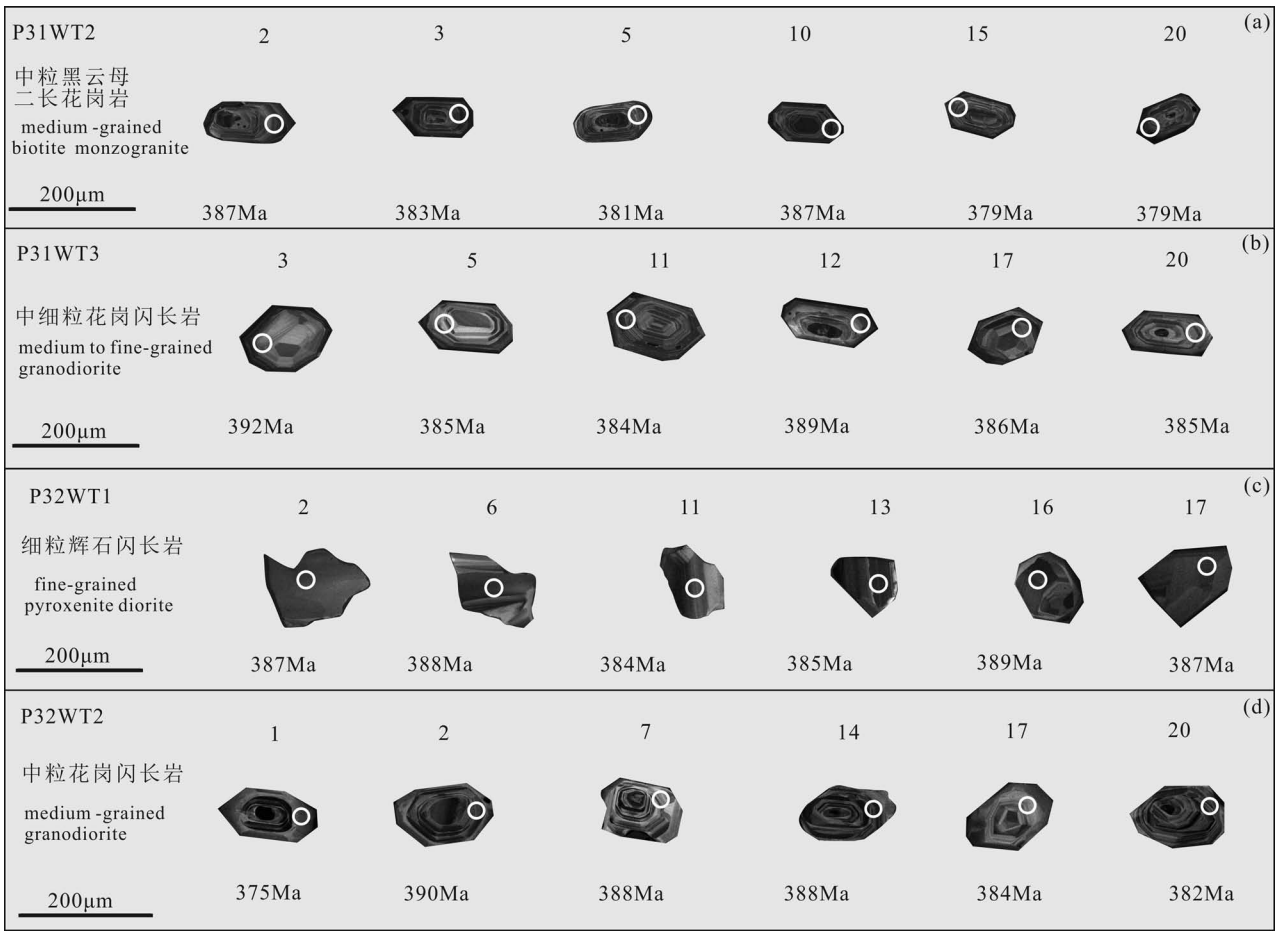


图 4 北山石板井地区侵入杂岩锆石 CL 图像

Fig. 4 CL images of the zircons from the granite in Shibanjing area, Beishan Mountains

中粒花岗闪长岩(P32WT2)锆石晶体粒径大小不一,一般为 100~150μm, 长宽比多数为 1.2∶1~2∶1,少数可达 2.5∶1。CL 图像显示(图 4d),内部振荡环带结构发育。对 19 粒锆石的分析结果表明,$n(^{206}Pb)/n(^{238}U)$表面年龄变化在 376~392 Ma(表 1,图 5h),其 $n(^{206}Pb)/n(^{238}U)$加权平均年龄为 385.5±1.1 Ma($n$=19,MSWD=10.7,图 5g),表明中粒花岗闪长岩结晶年龄为 385 Ma 左右。

### 3.2　岩石地球化学特征

#### 3.2.1　主量元素特征

从表 2 可知,所测花岗闪长岩的 $SiO_2$ 含量为 62.82%~68.68%、$Al_2O_3$ 含量为 13.57%~16.27%,$K_2O/Na_2O$ 比值为 0.29~0.80,里特曼指数(σ)为 2.28~2.38、分异指数($DI$)为 62.80~74.85,在 TAS 分类图解中位于花岗闪长岩区(图 6a)、高钾钙碱性—钙碱性(图 6b)、钠质—钾质(图 6c)、岩石的 A/CNK 值为 0.92~1.00,为准铝质系列(图 6d)岩石特征,其中中粒花岗闪长岩全部落在钙碱性区域内,属钠质岩石;二长花岗岩 $SiO_2$ 含量为 70.20%~71.84%、$Al_2O_3$ 含量为 13.67%~13.92%、$K_2O/Na_2O$ 值为 0.93~1.00,里特曼指数(σ)为 1.78~1.92、分异指数($DI$)为 82.18~84.15,在 TAS 分类图解中位于二长花岗质岩区(图 6a)、高钾钙碱性(图 6b)、钾质(图 6c)、岩石的 A/CNK 值为 1.01~1.04,为过铝质系列岩石(图 6d);

辉石闪长岩的 $SiO_2$ 含量为 53.56%~55.24%、$Al_2O_3$ 含量为 15.22%~16.29%、$Fe_2O_3$ 含量为 1.10%~1.50%、FeO 含量为 7.01%~7.08%、$K_2O/Na_2O$ 值为 0.22~0.27,里特曼指数(σ)为 1.61~2.10、分异指数($DI$)为 38.37~41.71,在 TAS 分类图解中位于呈现辉石闪长质岩区(图 6a)、钙碱性(图 6b)、钠质(图 6c)、岩石的 A/CNK 值为 0.67~0.71,为准铝质系列岩石(图 6d)。

上述岩石在哈克图解上,从细粒辉石闪长岩

**表 1 北山石坂井地区中酸性侵入杂岩 LA-ICP-MS 锆石 U-Pb 年龄分析结果**

**Table 1 Zircon LA-ICP-MS U-Pb dating of the intermediate—acidic intrusive complexes in Shibanjing area, Beishan Mountains**

| 测点号 | 元素含量($\times10^{-6}$) | | | Th/U | 同位素比值 | | | | | | 同位素年龄(Ma) | | | | | | 谐和度(%) |
|---|---|---|---|---|---|---|---|---|---|---|---|---|---|---|---|---|---|
| | Pb | Th | U | | $n(^{207}Pb)/n(^{206}Pb)$ | | $n(^{207}Pb)/n(^{235}U)$ | | $n(^{206}Pb)/n(^{238}U)$ | | $n(^{207}Pb)/n(^{206}Pb)$ | | $n(^{207}Pb)/n(^{235}U)$ | | $n(^{206}Pb)/n(^{238}U)$ | | |
| | | | | | 测值 | 1σ | 测值 | 1σ | 测值 | 1σ | 测值 | 1σ | 测值 | 1σ | 测值 | 1σ | |
| 中粒黑云母二长花岗岩(样品号 P31TW2) | | | | | | | | | | | | | | | | | |
| 1 | 16.6 | 137.3 | 224.2 | 0.61 | 0.05446 | 0.0014 | 0.4630 | 0.0115 | 0.06199 | 0.0006 | 390.8 | 62.0 | 386.3 | 8.0 | 387.7 | 3.9 | 99 |
| 2 | 12.8 | 86.9 | 178.2 | 0.49 | 0.05442 | 0.0015 | 0.4626 | 0.0126 | 0.06192 | 0.0006 | 387.1 | 63.0 | 386.0 | 8.7 | 387.3 | 3.9 | 99 |
| 3 | 18.2 | 150.9 | 249.5 | 0.60 | 0.05539 | 0.0012 | 0.4633 | 0.0093 | 0.06115 | 0.0007 | 427.8 | 43.5 | 386.6 | 6.4 | 382.6 | 4.1 | 98 |
| 4 | 14.2 | 93.3 | 202.6 | 0.46 | 0.05393 | 0.0015 | 0.4536 | 0.0125 | 0.06115 | 0.0006 | 368.6 | 61.1 | 379.8 | 8.7 | 382.6 | 3.7 | 99 |
| 5 | 17.3 | 128.1 | 241.0 | 0.53 | 0.05472 | 0.0012 | 0.4577 | 0.0102 | 0.06088 | 0.0006 | 466.7 | 50.0 | 382.7 | 7.1 | 380.9 | 3.6 | 99 |
| 6 | 14.0 | 95.2 | 198.1 | 0.48 | 0.05544 | 0.0014 | 0.4624 | 0.0123 | 0.06052 | 0.0006 | 431.5 | 57.4 | 385.9 | 8.5 | 378.8 | 3.8 | 98 |
| 7 | 15.0 | 86.8 | 210.6 | 0.41 | 0.05458 | 0.0023 | 0.4606 | 0.0211 | 0.06098 | 0.0011 | 394.5 | 94.4 | 384.7 | 14.7 | 381.6 | 6.8 | 99 |
| 8 | 16.9 | 113.6 | 230.8 | 0.49 | 0.05566 | 0.0048 | 0.4678 | 0.0428 | 0.06089 | 0.0013 | 438.9 | 194.4 | 389.7 | 29.6 | 381.0 | 7.8 | 97 |
| 9 | 20.3 | 141.8 | 288.3 | 0.49 | 0.05566 | 0.0013 | 0.4649 | 0.0104 | 0.06070 | 0.0006 | 438.9 | 50.0 | 387.6 | 7.2 | 379.9 | 3.5 | 97 |
| 10 | 17.8 | 164.4 | 236.6 | 0.69 | 0.05387 | 0.0014 | 0.4602 | 0.0124 | 0.06190 | 0.0007 | 364.9 | 55.6 | 384.4 | 8.6 | 387.1 | 4.3 | 99 |
| 11 | 17.7 | 151.0 | 242.0 | 0.62 | 0.05488 | 0.0015 | 0.4661 | 0.0131 | 0.06159 | 0.0007 | 405.6 | 65.7 | 388.5 | 9.1 | 385.3 | 4.2 | 99 |
| 12 | 11.4 | 94.4 | 162.0 | 0.58 | 0.05550 | 0.0022 | 0.4627 | 0.0194 | 0.06019 | 0.0007 | 431.5 | 87.0 | 386.1 | 13.5 | 376.8 | 4.4 | 97 |
| 13 | 7.8 | 64.3 | 111.1 | 0.58 | 0.05450 | 0.0018 | 0.4524 | 0.0148 | 0.06045 | 0.0007 | 390.8 | 71.3 | 379.0 | 10.4 | 378.3 | 4.0 | 99 |
| 14 | 17.0 | 117.0 | 244.1 | 0.48 | 0.05363 | 0.0011 | 0.4536 | 0.0098 | 0.06116 | 0.0005 | 353.8 | 78.7 | 379.8 | 6.9 | 382.7 | 3.2 | 99 |
| 15 | 15.1 | 121.5 | 215.1 | 0.56 | 0.05589 | 0.0015 | 0.4656 | 0.0118 | 0.06061 | 0.0006 | 455.6 | 59.3 | 388.1 | 8.1 | 379.3 | 3.6 | 97 |
| 16 | 13.1 | 97.1 | 188.8 | 0.51 | 0.05416 | 0.0015 | 0.4503 | 0.0122 | 0.06041 | 0.0006 | 376.0 | 58.3 | 377.5 | 8.5 | 378.1 | 3.6 | 99 |
| 17 | 15.9 | 126.9 | 226.1 | 0.56 | 0.05390 | 0.0014 | 0.4526 | 0.0114 | 0.06108 | 0.0005 | 368.6 | 63.9 | 379.1 | 8.0 | 382.2 | 3.2 | 99 |
| 18 | 20.6 | 159.9 | 294.9 | 0.54 | 0.05458 | 0.0012 | 0.4575 | 0.0094 | 0.06094 | 0.0006 | 394.5 | 48.1 | 382.5 | 6.6 | 381.4 | 3.8 | 99 |
| 20 | 15.9 | 127.5 | 226.7 | 0.56 | 0.05499 | 0.0018 | 0.4598 | 0.0150 | 0.06057 | 0.0006 | 413.0 | 69.4 | 384.1 | 10.4 | 379.1 | 3.6 | 98 |
| 中细粒花岗闪长岩(样品号 P31TW3) | | | | | | | | | | | | | | | | | |
| 1 | 17.0 | 134.5 | 223.4 | 0.60 | 0.05413 | 0.0015 | 0.4700 | 0.0132 | 0.06283 | 0.0006 | 376.0 | 58.3 | 391.2 | 9.1 | 392.8 | 3.7 | 99 |
| 2 | 11.7 | 90.1 | 161.7 | 0.56 | 0.05474 | 0.0024 | 0.4613 | 0.0203 | 0.06131 | 0.0009 | 466.7 | 100.0 | 385.2 | 14.1 | 383.6 | 5.5 | 99 |
| 3 | 9.1 | 79.8 | 119.5 | 0.67 | 0.05315 | 0.0018 | 0.4585 | 0.0158 | 0.06262 | 0.0008 | 344.5 | 75.9 | 383.2 | 11.0 | 391.5 | 4.7 | 97 |
| 4 | 12.1 | 80.1 | 169.4 | 0.47 | 0.05540 | 0.0014 | 0.4672 | 0.0121 | 0.06131 | 0.0007 | 427.8 | 55.6 | 389.3 | 8.4 | 383.6 | 4.0 | 98 |
| 5 | 9.9 | 64.9 | 139.7 | 0.46 | 0.05514 | 0.0020 | 0.4658 | 0.0170 | 0.06156 | 0.0008 | 416.7 | 75.0 | 388.3 | 11.8 | 385.1 | 5.1 | 99 |
| 7 | 12.9 | 128.6 | 176.8 | 0.73 | 0.05592 | 0.0022 | 0.4661 | 0.0175 | 0.06062 | 0.0007 | 450.0 | 119.4 | 388.5 | 12.1 | 379.4 | 4.2 | 97 |
| 8 | 11.0 | 73.0 | 146.4 | 0.50 | 0.05619 | 0.0024 | 0.4781 | 0.0194 | 0.06216 | 0.0011 | 461.2 | 94.4 | 396.8 | 13.3 | 388.7 | 6.6 | 97 |
| 9 | 13.4 | 103.1 | 178.9 | 0.58 | 0.05701 | 0.0017 | 0.4817 | 0.0135 | 0.06147 | 0.0007 | 500.0 | 66.7 | 399.2 | 9.3 | 384.6 | 4.1 | 96 |
| 10 | 15.2 | 134.4 | 198.0 | 0.68 | 0.05581 | 0.0014 | 0.4749 | 0.0128 | 0.06159 | 0.0006 | 455.6 | 57.4 | 394.6 | 8.8 | 385.3 | 3.8 | 97 |
| 11 | 17.7 | 148.6 | 239.9 | 0.62 | 0.05640 | 0.0016 | 0.4779 | 0.0138 | 0.06141 | 0.0005 | 477.8 | 32.4 | 396.7 | 9.5 | 384.2 | 3.2 | 96 |
| 12 | 12.1 | 101.7 | 162.8 | 0.62 | 0.05440 | 0.0012 | 0.4671 | 0.0108 | 0.06218 | 0.0005 | 387.1 | 47.2 | 389.2 | 7.5 | 388.9 | 3.1 | 99 |

| 测点号 | 元素含量(×10$^{-6}$) | | | Th/U | 同位素比值 | | | | | | 同位素年龄(Ma) | | | | | | 谐和度(%) |
|---|---|---|---|---|---|---|---|---|---|---|---|---|---|---|---|---|---|
| | Pb | Th | U | | $n(^{207}Pb)/n(^{206}Pb)$ | | $n(^{207}Pb)/n(^{235}U)$ | | $n(^{206}Pb)/n(^{238}U)$ | | $n(^{207}Pb)/n(^{206}Pb)$ | | $n(^{207}Pb)/n(^{235}U)$ | | $n(^{206}Pb)/n(^{238}U)$ | | |
| | | | | | 测值 | 1σ | 测值 | 1σ | 测值 | 1σ | 测值 | 1σ | 测值 | 1σ | 测值 | 1σ | |
| 13 | 12.7 | 106.8 | 173.6 | 0.62 | 0.05502 | 0.0028 | 0.4669 | 0.0240 | 0.06174 | 0.0008 | 413.0 | 111.1 | 389.1 | 16.6 | 386.2 | 5.0 | 99 |
| 14 | 15.5 | 116.1 | 215.6 | 0.54 | 0.05434 | 0.0013 | 0.4640 | 0.0115 | 0.06181 | 0.0004 | 383.4 | 55.6 | 387.0 | 8.0 | 386.6 | 2.7 | 99 |
| 16 | 20.3 | 219.8 | 272.8 | 0.81 | 0.05712 | 0.0014 | 0.4834 | 0.0126 | 0.06151 | 0.0006 | 494.5 | 53.7 | 400.4 | 8.6 | 384.8 | 3.8 | 96 |
| 17 | 11.9 | 100.9 | 164.0 | 0.62 | 0.05720 | 0.0018 | 0.4907 | 0.0173 | 0.06176 | 0.0007 | 498.2 | 70.4 | 405.4 | 11.8 | 386.3 | 4.1 | 95 |
| 20 | 11.3 | 98.7 | 157.1 | 0.63 | 0.05598 | 0.0018 | 0.4777 | 0.0161 | 0.06157 | 0.0006 | 450.0 | 65.7 | 396.5 | 11.0 | 385.2 | 3.6 | 97 |
| 细粒辉石闪长岩(样品号 P32TW1) | | | | | | | | | | | | | | | | | |
| 1 | 17.3 | 102.9 | 250.0 | 0.41 | 0.05689 | 0.0019 | 0.4774 | 0.0163 | 0.06102 | 0.0007 | 487.1 | 75.9 | 396.3 | 11.2 | 381.8 | 4.5 | 96 |
| 2 | 12.1 | 74.6 | 169.9 | 0.44 | 0.05437 | 0.0025 | 0.4627 | 0.0208 | 0.06191 | 0.0008 | 387.1 | 103.7 | 386.1 | 14.4 | 387.2 | 5.0 | 99 |
| 3 | 16.3 | 145.5 | 216.8 | 0.67 | 0.05665 | 0.0017 | 0.4750 | 0.0126 | 0.06133 | 0.0007 | 479.7 | 66.7 | 394.6 | 8.7 | 383.7 | 4.3 | 97 |
| 4 | 11.8 | 74.0 | 166.8 | 0.44 | 0.05532 | 0.0017 | 0.4639 | 0.0140 | 0.06121 | 0.0007 | 433.4 | 73.1 | 387.0 | 9.7 | 383.0 | 4.2 | 98 |
| 5 | 10.4 | 54.1 | 150.8 | 0.36 | 0.05650 | 0.0019 | 0.4736 | 0.0159 | 0.06100 | 0.0008 | 472.3 | 75.9 | 393.6 | 11.0 | 381.7 | 4.6 | 96 |
| 6 | 14.1 | 110.0 | 187.2 | 0.59 | 0.05515 | 0.0014 | 0.4709 | 0.0126 | 0.06199 | 0.0007 | 416.7 | 57.4 | 391.8 | 8.7 | 387.7 | 4.3 | 98 |
| 7 | 14.8 | 91.2 | 204.2 | 0.45 | 0.05498 | 0.0021 | 0.4702 | 0.0186 | 0.06203 | 0.0007 | 413.0 | 88.9 | 391.3 | 12.8 | 388.0 | 4.1 | 99 |
| 8 | 7.9 | 45.9 | 109.6 | 0.42 | 0.05735 | 0.0030 | 0.4765 | 0.0227 | 0.06086 | 0.0010 | 505.6 | 113.7 | 395.7 | 15.6 | 380.8 | 5.9 | 96 |
| 9 | 31.3 | 257.9 | 409.9 | 0.63 | 0.05565 | 0.0011 | 0.4735 | 0.0101 | 0.06175 | 0.0006 | 438.9 | 46.3 | 393.6 | 7.0 | 386.3 | 3.5 | 98 |
| 10 | 16.4 | 114.5 | 229.9 | 0.50 | 0.05636 | 0.0017 | 0.4707 | 0.0146 | 0.06088 | 0.0008 | 464.9 | 66.7 | 391.7 | 10.1 | 380.9 | 4.6 | 97 |
| 11 | 19.2 | 168.9 | 252.9 | 0.67 | 0.05809 | 0.0019 | 0.4908 | 0.0167 | 0.06132 | 0.0008 | 531.5 | 75.0 | 405.4 | 11.4 | 383.6 | 5.0 | 94 |
| 12 | 15.6 | 103.6 | 211.3 | 0.49 | 0.05604 | 0.0019 | 0.4690 | 0.0154 | 0.06112 | 0.0009 | 453.8 | 69.4 | 390.5 | 10.7 | 382.5 | 5.7 | 97 |
| 13 | 21.8 | 143.6 | 293.6 | 0.49 | 0.05632 | 0.0015 | 0.4774 | 0.0134 | 0.06153 | 0.0008 | 464.9 | 57.4 | 396.3 | 9.2 | 384.9 | 4.9 | 97 |
| 14 | 16.5 | 104.0 | 224.0 | 0.46 | 0.05410 | 0.0015 | 0.4596 | 0.0123 | 0.06189 | 0.0006 | 376.0 | 56.5 | 384.0 | 8.5 | 387.1 | 3.8 | 99 |
| 15 | 11.8 | 88.4 | 156.2 | 0.57 | 0.05534 | 0.0018 | 0.4718 | 0.0152 | 0.06198 | 0.0006 | 433.4 | 72.2 | 392.5 | 10.5 | 387.7 | 3.9 | 98 |
| 16 | 22.5 | 193.3 | 296.9 | 0.65 | 0.05457 | 0.0020 | 0.4690 | 0.0181 | 0.06216 | 0.0007 | 394.5 | 83.3 | 390.5 | 12.5 | 388.7 | 4.1 | 99 |
| 17 | 13.1 | 80.6 | 184.2 | 0.44 | 0.05586 | 0.0015 | 0.4749 | 0.0130 | 0.06183 | 0.0006 | 455.6 | 61.1 | 394.6 | 8.9 | 386.7 | 3.6 | 97 |
| 18 | 15.6 | 137.3 | 210.5 | 0.65 | 0.05543 | 0.0015 | 0.4655 | 0.0128 | 0.06101 | 0.0006 | 427.8 | 59.3 | 388.1 | 8.9 | 381.8 | 3.9 | 98 |
| 19 | 10.0 | 66.6 | 139.0 | 0.48 | 0.05527 | 0.0017 | 0.4727 | 0.0144 | 0.06224 | 0.0006 | 433.4 | 75.0 | 393.1 | 10.0 | 389.3 | 3.9 | 99 |
| 20 | 12.5 | 98.5 | 170.8 | 0.58 | 0.05376 | 0.0015 | 0.4586 | 0.0131 | 0.06189 | 0.0007 | 361.2 | 61.1 | 383.3 | 9.1 | 387.1 | 4.2 | 99 |
| 21 | 19.8 | 182.9 | 265.2 | 0.69 | 0.05555 | 0.0013 | 0.4701 | 0.0115 | 0.06146 | 0.0006 | 435.2 | 49.1 | 391.3 | 7.9 | 384.5 | 3.8 | 98 |
| 中粒花岗闪长岩(样品号 P32TW2) | | | | | | | | | | | | | | | | | |
| 2 | 7.9 | 52.2 | 107.0 | 0.49 | 0.05397 | 0.0041 | 0.4642 | 0.0359 | 0.0624 | 0.0012 | 368.6 | 172.2 | 387.2 | 24.9 | 390.2 | 7.0 | 99 |
| 3 | 18.2 | 135.3 | 243.2 | 0.56 | 0.05513 | 0.0013 | 0.4729 | 0.0121 | 0.0622 | 0.0007 | 416.7 | 55.6 | 393.2 | 8.3 | 389.3 | 4.3 | 99 |
| 4 | 24.9 | 235.7 | 330.0 | 0.71 | 0.05896 | 0.0014 | 0.4920 | 0.0119 | 0.06239 | 0.0006 | 564.9 | 47.2 | 406.3 | 8.1 | 378.9 | 3.6 | 93 |
| 5 | 12.4 | 98.9 | 168.2 | 0.59 | 0.05503 | 0.0017 | 0.4683 | 0.0146 | 0.06225 | 0.0006 | 413.0 | 68.5 | 390.0 | 10.1 | 387.5 | 3.8 | 99 |
| 6 | 10.4 | 76.9 | 138.6 | 0.55 | 0.05523 | 0.0046 | 0.4742 | 0.0376 | 0.06054 | 0.0012 | 420.4 | 182.4 | 394.1 | 25.9 | 392.2 | 7.5 | 99 |
| 7 | 11.3 | 78.2 | 157.8 | 0.50 | 0.05600 | 0.0020 | 0.4772 | 0.0172 | 0.06196 | 0.0008 | 453.8 | 77.8 | 396.2 | 11.8 | 388.0 | 4.9 | 97 |

| 测点号 | 元素含量($\times10^{-6}$) | | | Th/U | 同位素比值 | | | | | | 同位素年龄(Ma) | | | | | | 谐和度(%) |
|---|---|---|---|---|---|---|---|---|---|---|---|---|---|---|---|---|---|
| | Pb | Th | U | | $n(^{207}Pb)/n(^{206}Pb)$ | | $n(^{207}Pb)/n(^{235}U)$ | | $n(^{206}Pb)/n(^{238}U)$ | | $n(^{207}Pb)/n(^{206}Pb)$ | | $n(^{207}Pb)/n(^{235}U)$ | | $n(^{206}Pb)/n(^{238}U)$ | | |
| | | | | | 测值 | 1σ | 测值 | 1σ | 测值 | 1σ | 测值 | 1σ | 测值 | 1σ | 测值 | 1σ | |
| 8 | 15.2 | 124.5 | 208.6 | 0.60 | 0.05416 | 0.0016 | 0.4634 | 0.0134 | 0.06273 | 0.0007 | 376.0 | 66.7 | 386.6 | 9.3 | 389.3 | 4.0 | 99 |
| 9 | 11.9 | 97.4 | 167.7 | 0.58 | 0.05663 | 0.0027 | 0.4745 | 0.0258 | 0.06204 | 0.0011 | 476.0 | 110.2 | 394.3 | 17.8 | 377.0 | 6.4 | 95 |
| 10 | 14.5 | 115.4 | 197.1 | 0.59 | 0.05501 | 0.0016 | 0.4739 | 0.0136 | 0.06225 | 0.0008 | 413.0 | 64.8 | 393.9 | 9.4 | 392.0 | 4.8 | 99 |
| 11 | 13.0 | 108.1 | 178.9 | 0.60 | 0.05668 | 0.0024 | 0.4742 | 0.0196 | 0.06115 | 0.0010 | 479.7 | 91.7 | 394.1 | 13.5 | 382.6 | 6.1 | 97 |
| 12 | 24.6 | 222.3 | 326.5 | 0.68 | 0.05557 | 0.0017 | 0.4700 | 0.0141 | 0.06144 | 0.0008 | 435.2 | 68.5 | 391.2 | 9.8 | 384.4 | 5.0 | 98 |
| 13 | 15.5 | 131.6 | 213.5 | 0.62 | 0.05653 | 0.0017 | 0.4755 | 0.0145 | 0.06099 | 0.0007 | 472.3 | 66.7 | 395.0 | 10.0 | 381.7 | 4.2 | 96 |
| 14 | 15.0 | 122.2 | 201.8 | 0.61 | 0.05399 | 0.0013 | 0.4599 | 0.0105 | 0.06200 | 0.0006 | 372.3 | 58.3 | 384.2 | 7.3 | 387.8 | 3.4 | 99 |
| 15 | 16.5 | 133.6 | 229.6 | 0.58 | 0.05685 | 0.0018 | 0.4792 | 0.0143 | 0.06145 | 0.0007 | 487.1 | 70.4 | 397.5 | 9.8 | 384.5 | 4.4 | 96 |
| 16 | 16.6 | 159.2 | 223.1 | 0.71 | 0.05410 | 0.0015 | 0.4624 | 0.0121 | 0.06224 | 0.0006 | 376.0 | 56.5 | 385.9 | 8.4 | 389.3 | 3.9 | 99 |
| 17 | 9.2 | 70.9 | 128.7 | 0.55 | 0.05659 | 0.0018 | 0.4772 | 0.0155 | 0.06131 | 0.0007 | 476.0 | 39.8 | 396.2 | 10.7 | 383.6 | 4.1 | 96 |
| 18 | 8.2 | 63.1 | 116.1 | 0.54 | 0.05535 | 0.0053 | 0.4595 | 0.0401 | 0.06109 | 0.0011 | 427.8 | 214.8 | 383.9 | 27.9 | 382.3 | 7.0 | 99 |
| 19 | 11.1 | 81.4 | 157.8 | 0.52 | 0.05695 | 0.0019 | 0.4795 | 0.0160 | 0.06116 | 0.0007 | 500.0 | 72.2 | 397.7 | 11.0 | 382.7 | 4.5 | 96 |
| 20 | 11.1 | 104.3 | 151.8 | 0.69 | 0.05629 | 0.0019 | 0.4733 | 0.0165 | 0.06105 | 0.0008 | 464.9 | 75.9 | 393.4 | 11.4 | 382.0 | 4.7 | 97 |

**表 2 北山石板井地区中酸性侵入杂岩的主量(%)、微量元素($\times10^{-6}$)和稀土元素($\times10^{-6}$)分析结果**

**Table 2 The analytical results of major(%), trace elements($\times10^{-6}$) and rare earth elements($\times10^{-6}$) for the intermediate—acidic intrusive in Shibanjing area, Beishan Mountains**

| 样品号 | P32YQ1 | P32YQ2 | P32YQ3 | P32YQ4 | P32YQ6 | P32YQ7 | P32YQ8 | P32YQ9 | P31YQ1 | P31YQ2 | P31YQ3 | P31YQ4 | P31YQ5 | P31YQ6 | P31YQ7 | P31YQ8 | P31YQ9 |
|---|---|---|---|---|---|---|---|---|---|---|---|---|---|---|---|---|---|
| 岩 性 | 细粒辉石闪长岩 | | | 中粒花岗闪长岩 | | | | | 中细粒花岗闪长岩 | | | 中粒黑云母二长花岗岩 | | | 中细粒花岗闪长岩 | | |
| $SiO_2$ | 53.56 | 55.24 | 54.44 | 62.82 | 66.36 | 63.74 | 63.86 | 64.36 | 66.44 | 66.68 | 68.68 | 71.84 | 70.48 | 70.20 | 68.04 | 66.82 | 65.40 |
| $Al_2O_3$ | 16.29 | 15.44 | 15.22 | 16.27 | 14.72 | 15.77 | 15.37 | 15.59 | 14.12 | 14.59 | 13.57 | 13.67 | 13.92 | 13.91 | 14.44 | 14.82 | 15.02 |
| $Fe_2O_3$ | 1.10 | 1.49 | 1.50 | 1.13 | 1.03 | 1.66 | 0.91 | 1.25 | 1.31 | 1.34 | 1.58 | 1.23 | 1.46 | 1.22 | 1.09 | 1.11 | 1.39 |
| FeO | 7.08 | 7.01 | 7.08 | 4.63 | 4.25 | 4.41 | 5.56 | 4.54 | 4.38 | 4.25 | 3.76 | 1.77 | 1.74 | 2.38 | 3.25 | 3.25 | 3.99 |
| MnO | 0.13 | 0.15 | 0.15 | 0.09 | 0.08 | 0.09 | 0.10 | 0.09 | 0.09 | 0.08 | 0.08 | 0.05 | 0.05 | 0.05 | 0.07 | 0.07 | 0.08 |
| $TiO_2$ | 1.1 | 1.1 | 1.08 | 0.89 | 0.84 | 1.08 | 1.12 | 0.90 | 1.00 | 1.00 | 0.84 | 0.46 | 0.49 | 0.54 | 0.68 | 0.74 | 0.77 |
| CaO | 8.65 | 8.48 | 8.55 | 4.78 | 3.94 | 4.52 | 4.19 | 4.29 | 3.51 | 3.50 | 3.04 | 1.84 | 2.16 | 2.00 | 2.87 | 3.27 | 3.42 |
| MgO | 5.62 | 4.79 | 4.92 | 1.98 | 1.91 | 1.70 | 1.89 | 1.86 | 1.68 | 1.61 | 1.44 | 0.75 | 0.86 | 0.80 | 1.54 | 1.60 | 1.86 |
| $Na_2O$ | 3.84 | 3.70 | 3.70 | 4.39 | 3.84 | 4.21 | 4.19 | 4.30 | 3.84 | 3.78 | 3.61 | 3.59 | 3.72 | 3.67 | 3.68 | 3.82 | 3.70 |
| $K_2O$ | 0.83 | 0.83 | 0.99 | 1.27 | 1.64 | 1.93 | 2.08 | 1.79 | 2.08 | 2.33 | 2.57 | 3.59 | 3.45 | 3.59 | 2.96 | 2.78 | 2.95 |
| $P_2O_5$ | 0.22 | 0.08 | 0.08 | 0.22 | 0.18 | 0.21 | 0.23 | 0.21 | 0.19 | 0.18 | 0.18 | 0.09 | 0.10 | 0.11 | 0.14 | 0.13 | 0.17 |
| LOS | 1.38 | 0.99 | 1.39 | 0.88 | 1.06 | 0.74 | 0.67 | 0.63 | 0.94 | 0.96 | 0.77 | 0.73 | 0.80 | 0.80 | 0.95 | 0.74 | 0.93 |
| Σ | 99.8 | 99.3 | 99.1 | 99.4 | 99.9 | 100.1 | 100.2 | 99.8 | 99.6 | 100.3 | 100.1 | 99.6 | 99.2 | 99.3 | 99.7 | 99.2 | 99.7 |
| σ | 2.10 | 1.61 | 1.81 | 1.59 | 1.27 | 1.81 | 1.88 | 1.72 | 1.48 | 1.57 | 1.48 | 1.78 | 1.86 | 1.92 | 1.75 | 1.81 | 1.95 |

| 样品号 | P32YQ1 | P32YQ2 | P32YQ3 | P32YQ4 | P32YQ6 | P32YQ7 | P32YQ8 | P32YQ9 | P31YQ1 | P31YQ2 | P31YQ3 | P31YQ4 | P31YQ5 | P31YQ6 | P31YQ7 | P31YQ8 | P31YQ9 |
|---|---|---|---|---|---|---|---|---|---|---|---|---|---|---|---|---|---|
| 岩 性 | 细粒辉石闪长岩 | | | 中粒花岗闪长岩 | | | | | 中细粒花岗闪长岩 | | | 中粒黑云母二长花岗岩 | | | 中细粒花岗闪长岩 | | |
| $K_2O/Na_2O$ | 0.22 | 0.22 | 0.27 | 0.29 | 0.43 | 0.46 | 0.50 | 0.42 | 0.54 | 0.62 | 0.71 | 1.00 | 0.93 | 0.98 | 0.80 | 0.73 | 0.80 |
| ACNK | 0.71 | 0.69 | 0.67 | 0.94 | 0.97 | 0.92 | 0.92 | 0.93 | 0.94 | 0.97 | 0.95 | 1.04 | 1.01 | 1.03 | 1.00 | 0.97 | 0.97 |
| DI | 38.37 | 41.71 | 41.36 | 62.80 | 67.33 | 65.88 | 65.30 | 66.24 | 70.01 | 70.20 | 73.96 | 84.15 | 82.38 | 82.18 | 74.85 | 73.02 | 70.23 |
| Cs | 2.33 | 1.88 | 2.66 | 3.28 | 5.52 | 4.66 | 6.94 | 5.31 | 4.79 | 5.52 | 4.39 | 4.82 | 6.23 | 7.27 | 6.48 | 5.71 | 6.69 |
| Ba | 221 | 241 | 292 | 309 | 434 | 422 | 456 | 397 | 615 | 510 | 616 | 423 | 475 | 563 | 489 | 509 | 506 |
| Hf | 6.28 | 2.85 | 5.25 | 8.28 | 6.53 | 6.30 | 8.16 | 7.73 | 10.90 | 7.32 | 11.00 | 7.12 | 7.25 | 8.90 | 6.66 | 7.27 | 8.51 |
| Ta | 0.48 | 0.51 | 0.58 | 0.72 | 0.70 | 0.71 | 0.90 | 0.91 | 0.88 | 0.84 | 0.92 | 0.76 | 0.72 | 0.92 | 0.84 | 0.78 | 0.95 |
| Th | 3.68 | 5.93 | 5.49 | 5.77 | 12.8 | 9.39 | 12.70 | 10.80 | 13.40 | 13.80 | 16.70 | 11.90 | 16.50 | 19.90 | 15.10 | 13.60 | 20.20 |
| U | 0.66 | 1.01 | 0.95 | 1.42 | 1.97 | 2.29 | 1.65 | 2.39 | 1.65 | 2.06 | 1.80 | 2.66 | 3.74 | 3.89 | 1.84 | 1.87 | 2.09 |
| Sn | 2.48 | 1.69 | 2.60 | 2.35 | 2.04 | 2.80 | 2.71 | 2.80 | 2.82 | 3.16 | 2.61 | 2.80 | 2.88 | 4.14 | 2.06 | 2.86 | 4.59 |
| V | 193 | 69 | 150 | 67 | 79 | 77 | 92 | 83 | 66 | 66 | 61 | 29 | 35 | 31 | 63 | 62 | 76 |
| Cr | 43.9 | 35.4 | 44.6 | 22.2 | 30.4 | 14.9 | 22.9 | 21.6 | 22.9 | 23.6 | 17.7 | 15.5 | 24.8 | 16.8 | 27.3 | 31.4 | 35.3 |
| Ni | 29.4 | 21.8 | 28.5 | 8.9 | 11.5 | 4.9 | 7.2 | 4.7 | 8.8 | 6.6 | 6.7 | 3.3 | 7.6 | 4.5 | 12.1 | 12.5 | 14.8 |
| Rb | 23.7 | 31.6 | 43.2 | 44.1 | 75.1 | 76.2 | 101 | 70.9 | 106 | 115 | 118 | 170 | 158 | 181 | 131 | 125 | 148 |
| Sr | 253 | 260 | 298 | 264 | 207 | 200 | 218 | 222 | 178 | 168 | 152 | 113 | 122 | 113 | 158 | 172 | 165 |
| Zr | 227 | 91 | 193 | 332 | 270 | 244 | 319 | 285 | 428 | 297 | 428 | 246 | 240 | 306 | 250 | 293 | 307 |
| Nb | 9.2 | 7.5 | 8.8 | 10.3 | 9.0 | 10.5 | 14.2 | 11.2 | 14.8 | 14.2 | 11.9 | 8.9 | 9.2 | 10.6 | 10.9 | 11.3 | 14.1 |
| Y | 46.3 | 36.8 | 31.9 | 32.1 | 27.1 | 36.6 | 39.3 | 34.5 | 53.4 | 45.9 | 50.6 | 34.2 | 35.0 | 43.2 | 32.5 | 32.3 | 39.7 |
| La | 24.3 | 15.8 | 15.5 | 25.5 | 23.1 | 28.1 | 34.6 | 29.5 | 41.4 | 34.5 | 53.9 | 25.8 | 41.7 | 44.9 | 38.7 | 27.7 | 48.4 |
| Ce | 59.1 | 34.9 | 32.3 | 52.7 | 44.9 | 58.2 | 68.8 | 58.3 | 89.6 | 75.3 | 112.0 | 57.3 | 83.3 | 90.8 | 75.1 | 63.3 | 99.7 |
| Pr | 8.27 | 4.86 | 4.81 | 6.89 | 5.93 | 7.28 | 8.38 | 7.24 | 11.30 | 9.97 | 13.60 | 6.93 | 9.74 | 10.60 | 8.85 | 7.23 | 11.10 |
| Nd | 36.5 | 22.2 | 21.3 | 30.8 | 25.8 | 30.0 | 35.1 | 30.5 | 47.2 | 42.5 | 56.3 | 28.9 | 37.4 | 40.8 | 34.9 | 30.3 | 40.2 |
| Sm | 8.39 | 5.84 | 5.39 | 6.75 | 5.83 | 6.68 | 7.34 | 6.37 | 10.30 | 9.48 | 11.10 | 6.35 | 7.41 | 8.21 | 7.01 | 6.03 | 8.39 |
| Eu | 1.87 | 1.66 | 1.66 | 1.73 | 1.73 | 1.62 | 1.65 | 1.66 | 1.62 | 1.64 | 1.65 | 1.05 | 1.160 | 1.14 | 1.37 | 1.45 | 1.61 |
| Gd | 7.92 | 6.07 | 5.17 | 6.40 | 5.35 | 6.46 | 7.23 | 5.76 | 9.61 | 8.62 | 9.79 | 5.77 | 6.45 | 7.81 | 6.15 | 5.66 | 7.06 |
| Tb | 1.39 | 1.18 | 0.99 | 1.09 | 0.92 | 1.17 | 1.19 | 1.10 | 1.79 | 1.56 | 1.80 | 1.03 | 1.16 | 1.33 | 1.05 | 1.04 | 1.28 |
| Dy | 8.06 | 6.98 | 5.77 | 6.06 | 4.93 | 6.42 | 6.73 | 6.12 | 9.94 | 8.68 | 9.81 | 6.13 | 6.52 | 7.64 | 5.48 | 5.75 | 6.97 |
| Ho | 1.79 | 1.41 | 1.22 | 1.24 | 1.14 | 1.41 | 1.46 | 1.41 | 2.00 | 1.83 | 2.01 | 1.29 | 1.38 | 1.63 | 1.21 | 1.19 | 1.45 |
| Er | 5.16 | 4.20 | 3.72 | 3.46 | 3.35 | 4.04 | 4.32 | 3.98 | 5.65 | 4.79 | 5.70 | 3.89 | 3.95 | 4.65 | 3.48 | 3.66 | 4.39 |
| Tm | 0.86 | 0.65 | 0.58 | 0.51 | 0.50 | 0.64 | 0.75 | 0.63 | 0.84 | 0.73 | 0.84 | 0.65 | 0.56 | 0.70 | 0.58 | 0.52 | 0.65 |
| Yb | 5.19 | 4.09 | 3.93 | 3.13 | 2.75 | 3.84 | 4.33 | 3.93 | 4.96 | 4.21 | 4.45 | 3.65 | 3.42 | 4.49 | 3.52 | 3.26 | 4.01 |
| Lu | 0.90 | 0.69 | 0.65 | 0.54 | 0.49 | 0.61 | 0.72 | 0.67 | 0.74 | 0.70 | 0.77 | 0.53 | 0.60 | 0.71 | 0.60 | 0.61 | 0.69 |
| ∑REE | 169.7 | 110.5 | 103.0 | 146.8 | 126.7 | 156.5 | 182.6 | 157.2 | 237.0 | 204.5 | 283.7 | 149.3 | 204.8 | 225.4 | 188.0 | 157.7 | 235.9 |
| LREE/HREE | 4.43 | 3.37 | 3.67 | 5.54 | 5.52 | 5.36 | 5.83 | 5.66 | 5.67 | 5.57 | 7.07 | 5.51 | 7.52 | 6.78 | 7.52 | 6.27 | 7.90 |
| $La_N/Yb_N$ | 3.16 | 2.60 | 2.66 | 5.49 | 5.66 | 4.93 | 5.39 | 5.06 | 5.63 | 5.52 | 8.17 | 4.77 | 8.22 | 6.74 | 7.41 | 5.73 | 8.14 |
| δEu | 0.69 | 0.85 | 0.95 | 0.79 | 0.93 | 0.74 | 0.68 | 0.82 | 0.49 | 0.54 | 0.47 | 0.52 | 0.50 | 0.43 | 0.62 | 0.75 | 0.62 |

⟶中粒花岗闪长岩⟶中细粒花岗闪长岩⟶中粒黑云母二长花岗岩具有同源岩浆演化的特征，即：随 $SiO_2$ 含量增加，$Al_2O_3$、$TiO_2$、TFeO、MgO 均呈现降低的趋势，而 $K_2O/Na_2O$ 和 $K_2O$ 呈现升高的趋势（图 7a—f）。

### 3.2.2 稀土和微量元素地球化学特征

从表 2 可知：中细粒花岗闪长岩的 ∑REE 为 $157.7\times10^{-6}\sim283.7\times10^{-6}$、$La_N/Yb_N$ 值为 5.52～8.17、δEu 为 0.47～0.75；中粒花岗闪长岩的 ∑REE 为 $126.7\times10^{-6}\sim182.6\times10^{-6}$、$La_N/Yb_N$ 值为 4.93～5.66、δEu 为 0.68～0.93；中粒黑云母二长花岗岩的

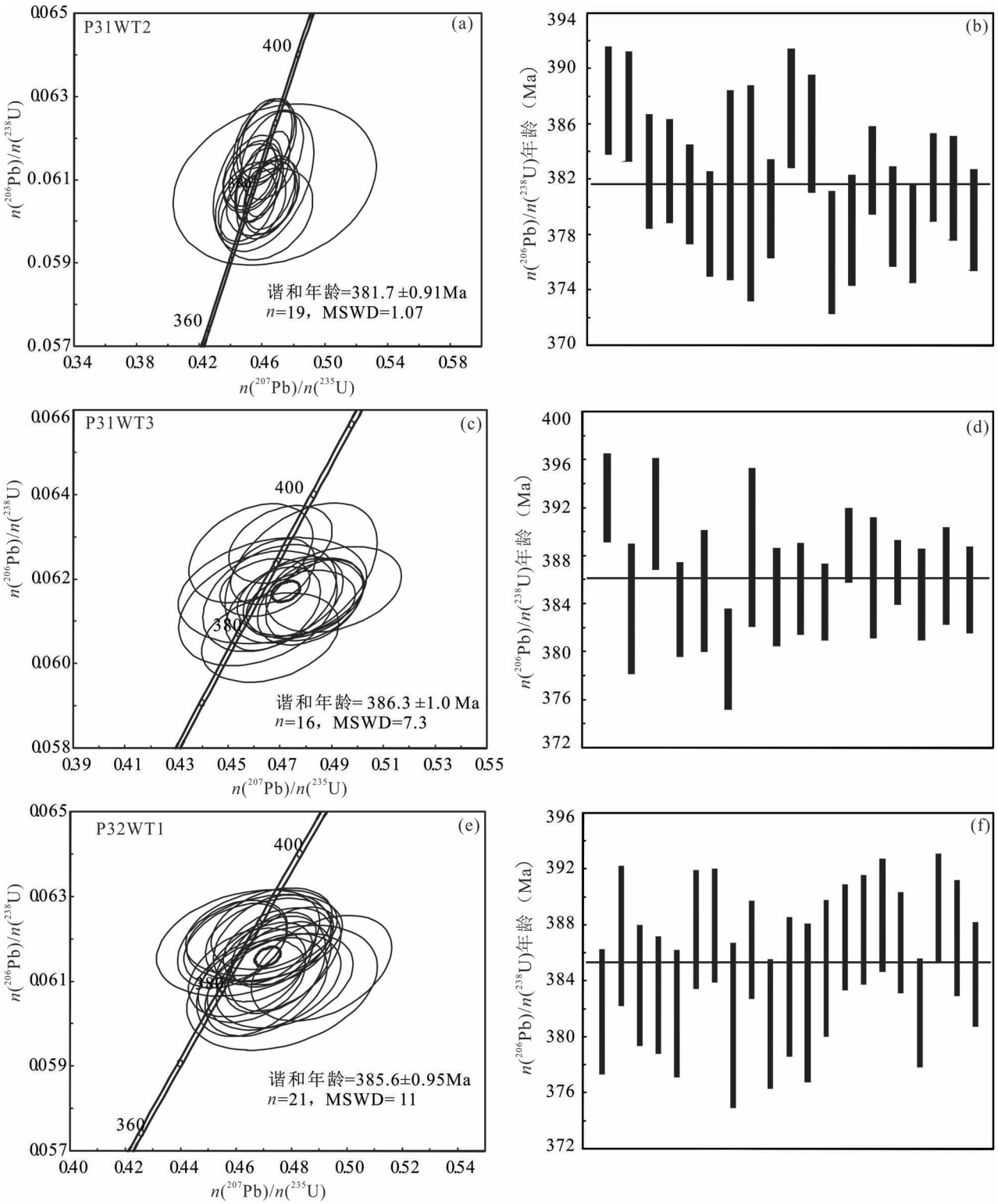

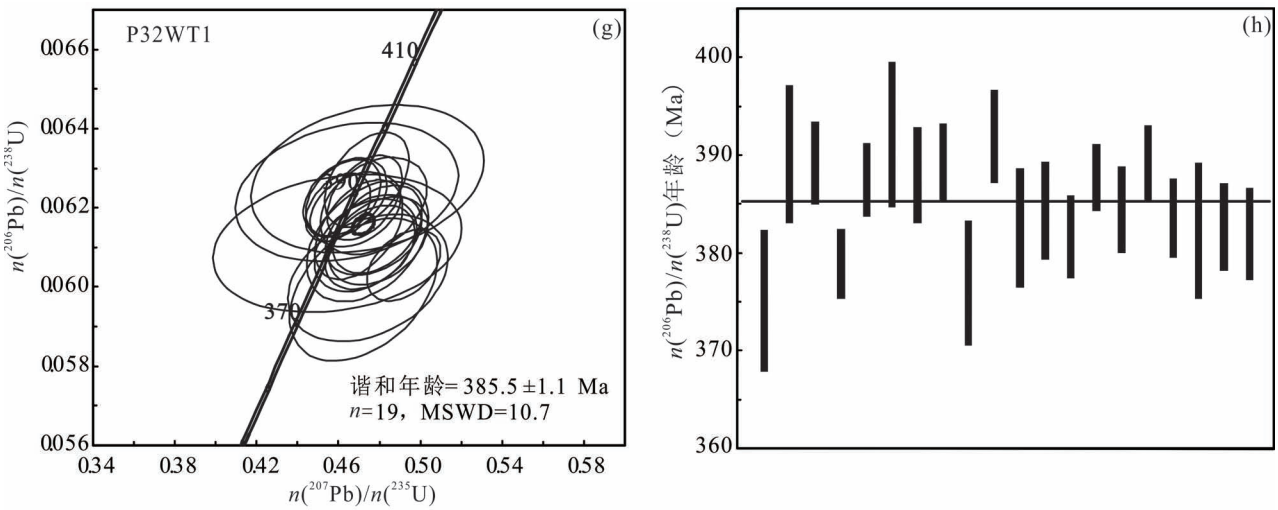


图 5 北山石板井地区侵入杂岩锆石 U-Pb 年龄图

Fig. 5 U-Pb concordia diagrams of the zircons from the granite in Shibanjing area, Beishan Mountains

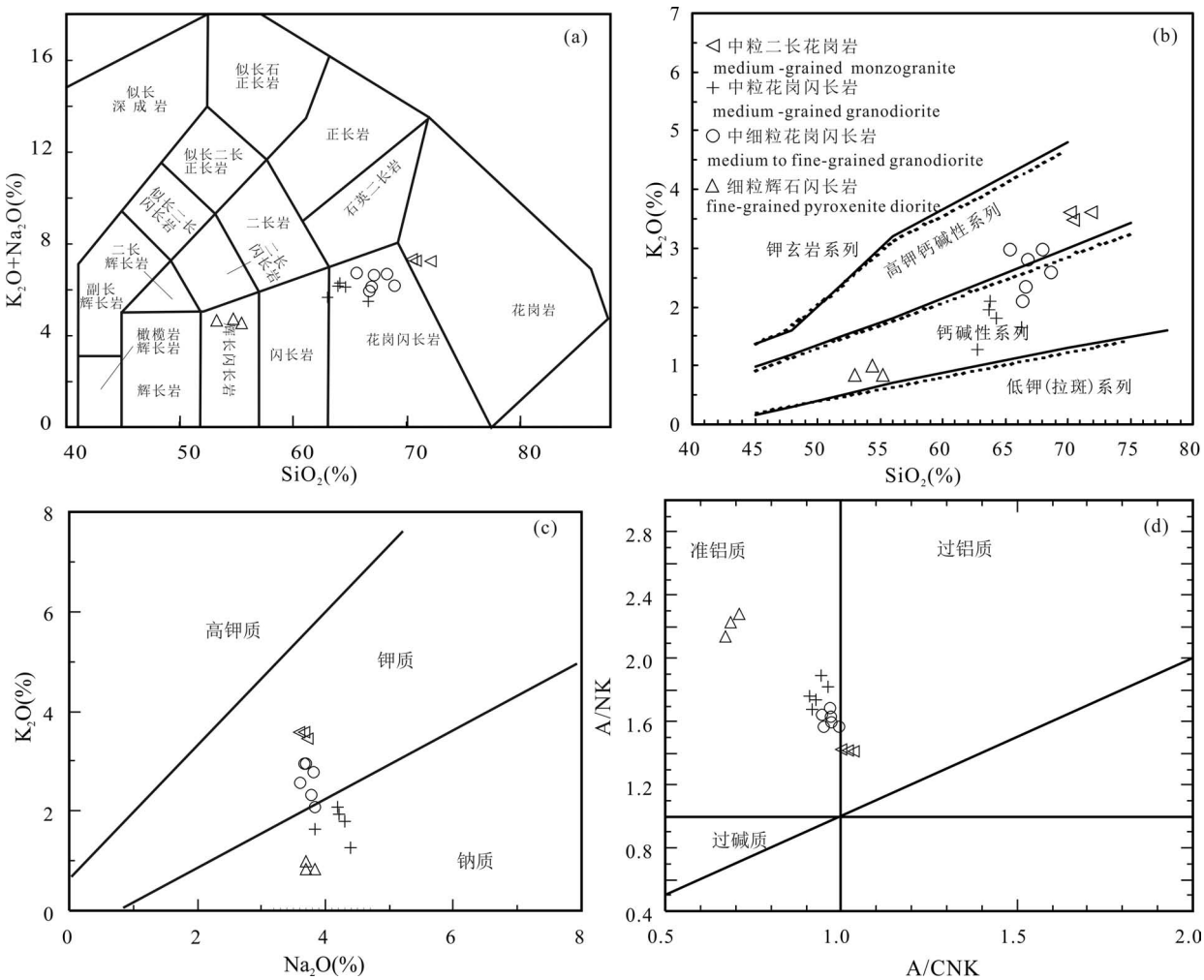


图 6 北山石板井地区中酸性侵入杂岩岩石分类图解(a)、$SiO_2$—$K_2O$ 岩石系列判别图解(b)、$K_2O$—$Na_2O$ 岩石系列判别图解(c)、A/CNK—A/NK 判别图解(d)

Fig. 6 Rock classification diagrams(a), $SiO_2$—$K_2O$ diagrams for rock series discrimination (b), $K_2O$—$Na_2O$ diagrams for rock series discrimination (c), A/CNK—A/NK diagrams(d) of the intrusive rocks in Shibanjing area, Beishan Mountains

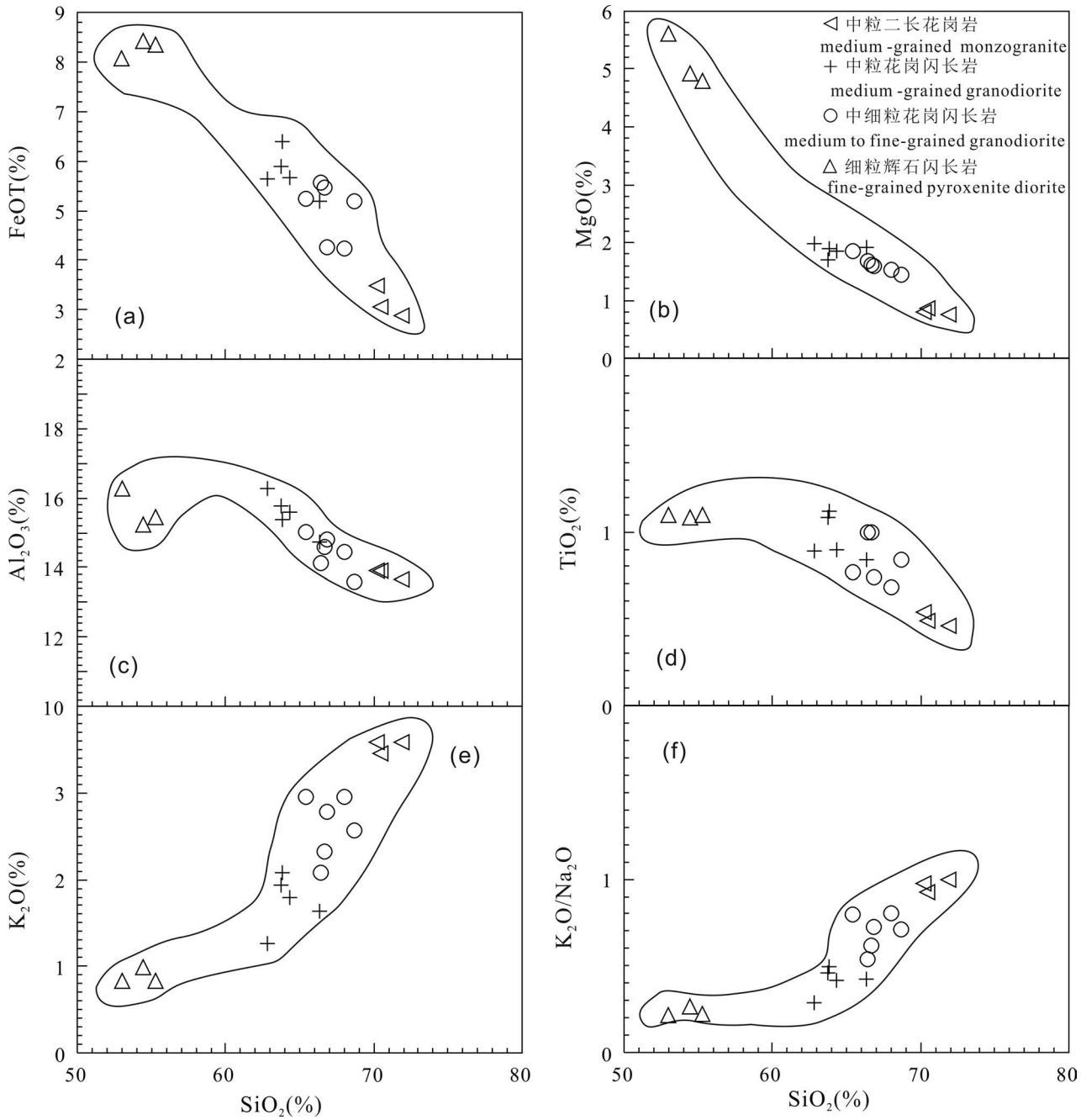


图 7 北山石板井地区侵入杂岩各类岩石 $SiO_2$ 与氧化物变异图

Fig. 7 Variation diagrams of $SiO_2$—oxides for the intrusive rocks in Shibanjing area, Beishan Mountains

∑REE 为 $149.3\times10^{-6}\sim225.4\times10^{-6}$、$La_N/Yb_N$ 值为 4.77~8.22、δEu 为 0.43~0.52；细粒辉石闪长岩的 ∑REE 为 $103.0\times10^{-6}\sim169.7\times10^{-6}$、$La_N/Yb_N$ 值为 2.60~3.16、δEu 为 0.69~0.95。在稀土元素对球粒陨石标准化图解上，4 类侵入岩均呈现富集轻稀土元素、相对亏损重稀土的配分形式，表现出不同程度的负铕异常，辉石闪长岩负异常相对较弱，二长花岗岩和花岗闪长岩相对富集 LREE 元素（图 8a、c）；在微量元素与原始地幔标准化图上，均呈现富集 Rb、Zr、Hf、Th、U 等元素，相对亏损 Nb、Ta、P、Ti、Sr、Ba 等元素，且二长花岗岩亏损 Ti、Sr 等元素程度相对较高（图 8b、d）；这种特征表明中细粒花岗闪长岩岩浆向中粒二长花岗岩浆演化过程发生了斜长石分离结晶作用。4 类岩石中，二长花岗岩相对富集 ∑REE、LREE/HREE、$La_N/Yb_N$（图 8c）和 Th、U 等元素（图 8d），相对亏损 Sr、P、Ti 等元素（图 8d）；中粒花

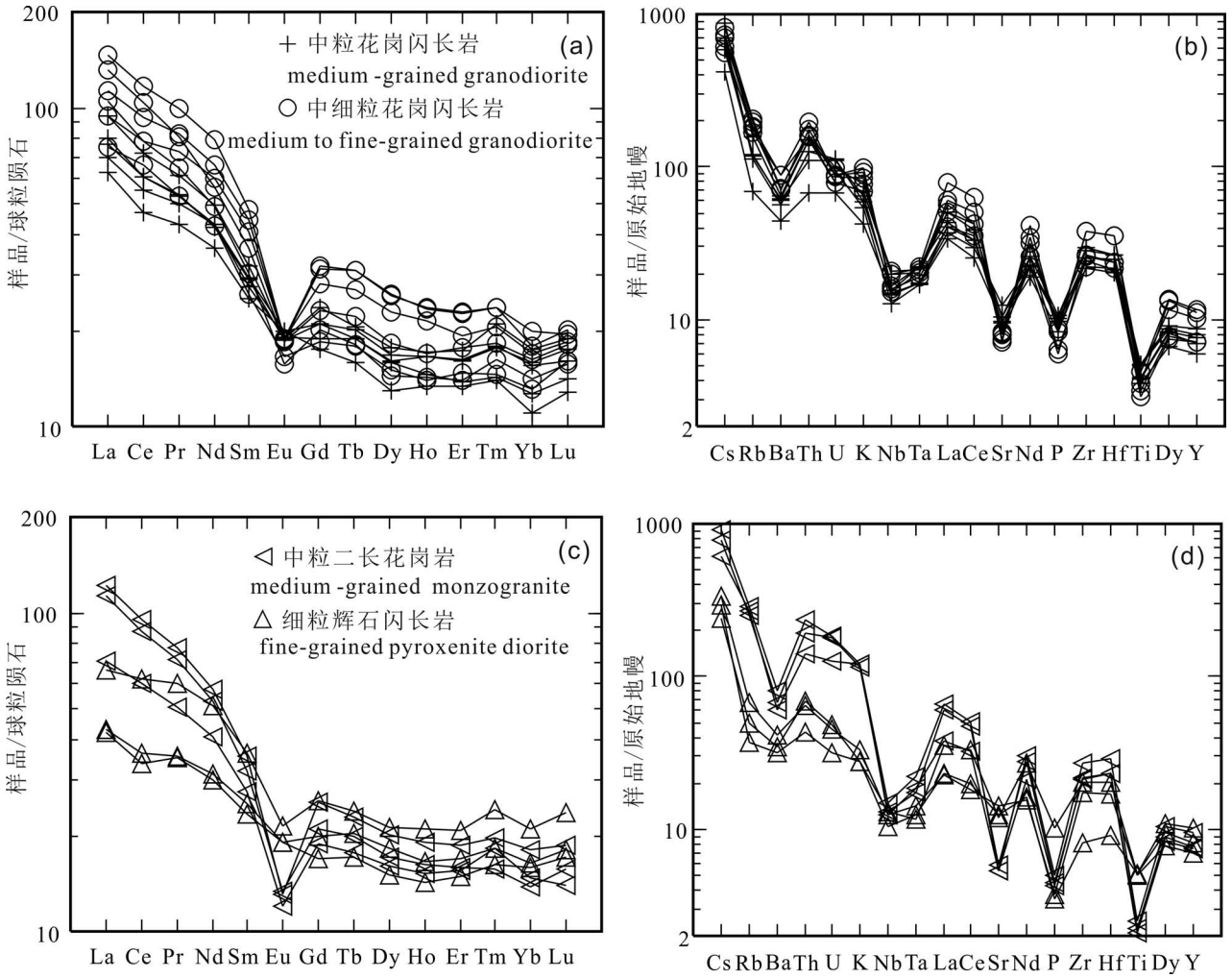


图 8 北山石板井地区侵入杂岩稀土配分模式(a、c)和微量元素对原始地幔(b、d)图解

Fig. 8 chondrite-normalized REE distribution pattern (a、c) and Primitive mantle normalized trace elements diagram (b、d) for the intrusive rocks in Shibanjing area, Beishan Mountains

岗闪长岩和中细粒花岗闪长岩具有相似的稀土和微量元素特征,所不同的是中细粒花岗闪长岩 LREE 相对富集(图 8a)。辉石闪长岩持有较低的 ∑REE 和弱的铕负异常(图 8c),明显亏损 Nb、Ta、P、Ti、Ba、Sr 和 LREE 等元素(图 8d)。

# 4　讨论

## 4.1　岩石成因

上述地质、年代学和地球化学特征表明,中粒黑云母二长花岗岩与中粒花岗闪长岩和中细粒花岗闪长岩岩石具有同源岩浆演化作用的特征,岩浆演化过程发生了斜长石分离结晶作用,同时 Sr、Ba、P、Ti 的亏损暗示了岩浆上升过程中发生了斜长石、黑云母、磷灰石、榍石等矿物的分离结晶作用,岩浆作用发生在中泥盆世(380~385 Ma);鉴于辉石闪长岩与花岗闪长岩时空关系上密切伴生,且微量元素具有明显的分离结晶趋势,可认为辉石闪长岩与花岗闪长岩是同源岩浆演化的结果(图 7d)。首先元素地球化学特征表明,二长花岗岩属高钾钙碱性、钾质、过铝质岩石(图 6b—d),花岗闪长岩属高钾钙碱性—钙碱性、钾质、准铝质岩石(图 6b—d),辉石闪长岩属钙碱性、钠质、准铝质岩石(图 6b—d);典型的 I 花岗岩 $Na_2O>3.2\%$,$K_2O/Na_2O<1.00$,$A/CNK<1.1$(Pitche, 1983; Chappell and White, 2001),本文中酸性侵入杂岩的 $Na_2O$ 含量为 3.61%~4.39%,$K_2O/Na_2O$ 为 0.22~1.00,A/CNK 为 0.67~1.04,以及岩相学特征均呈现 I 型花岗岩特征(表 2,图 9a),同时出现 I 花岗岩中典型矿物辉石和角闪石,进一

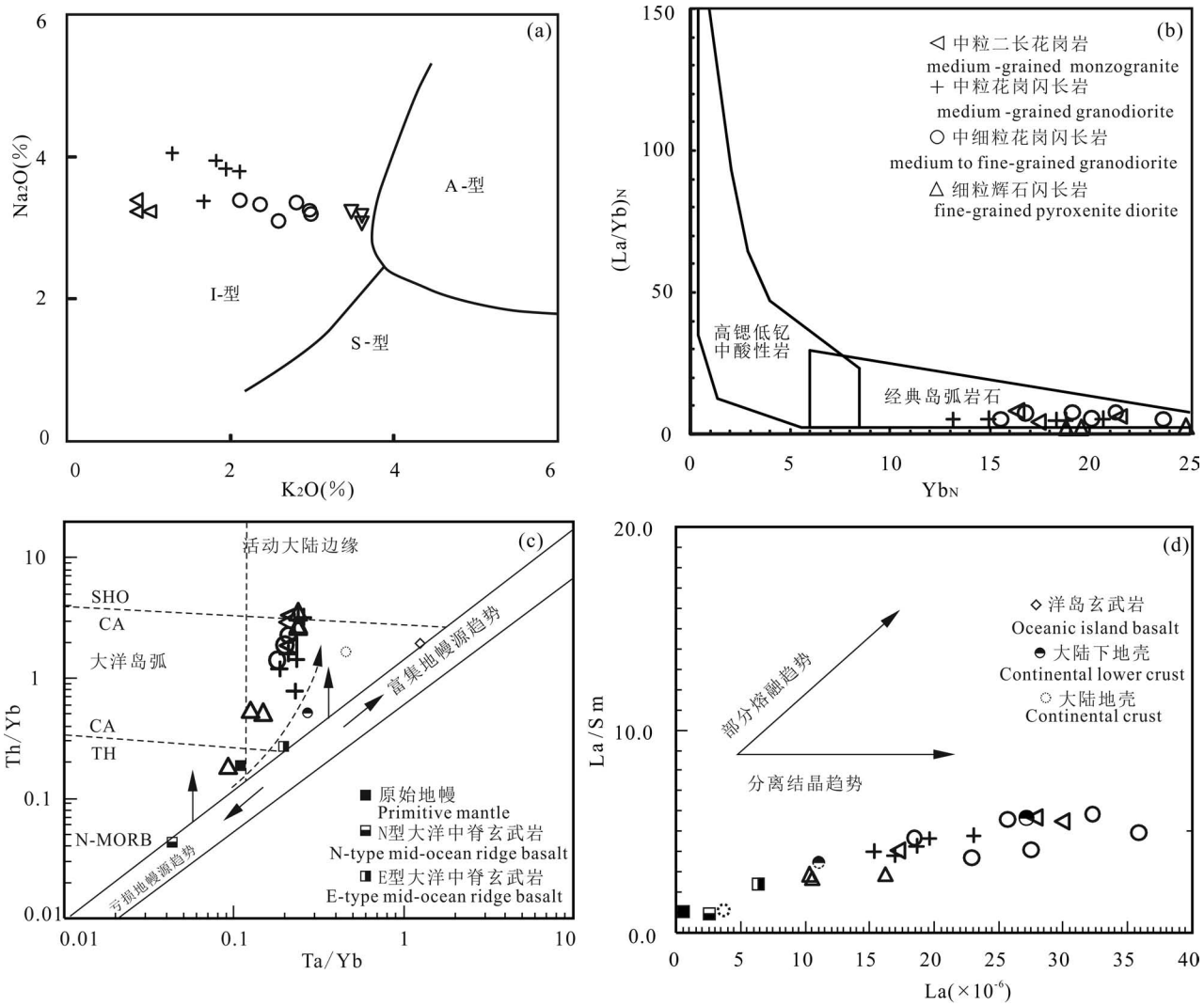


图 9 北山石板井地区侵入杂岩元素地球化学图解(底图据 Collins et al. ,1982;Defant and Drumrnond,1990)

Fig. 9 Elemental geochemistry diagram (base map from Collins et al. ,1982;Defant and Drumrnond,1990) for the intrusive rocks in Shibanjing area, Beishan Mountains

步证实其属于 I 型花岗岩(邓晋福等,2015a)。通过岩石组合初步判断为岛弧或大陆边缘弧构造环境(邓晋福等,2015b),岩石明显亏损 Nb、Tb、Ti、P、Sr 和有不同程度的铕负异常,在稀土元素对 N-MORB 图解上,与 N-MORB 相比,明显富集轻稀土和亏损重稀土元素(铕元素两侧)(图 8b、d),具有岛弧花岗岩的特征,反映其岩浆可能起源于俯冲板片流体交代的地幔楔;$Yb_N$ 与$(La/Yb)_N$ 图解中落入经典岛弧岩石区域(图 8c);在 Ta/Yb 与 Th/Yb 图解中落入大洋岛弧区(图 9b),其性质与三道明水花岗岩相近(张文,2013),表现为大洋岛弧花岗岩特征;该区邻区中粒辉长岩的锆石 U-Pb 年龄为 395.6±2.3 Ma(作者待发表),而在该侵入杂岩北侧出露有石板井—小黄山蛇绿混杂岩(杨合群等,2010;赵志雄等,2018),因此这些年轻地壳物质可能由洋壳或岛弧建造组成。大洋板片俯冲过程中流体交代了地幔楔,地幔楔部分熔融形成玄武质岩浆,玄武质岩浆底侵引起这些年轻地壳物质经部分熔融形成花岗质岩浆,并在该区形成具有大洋岛弧性质的花岗质岩石。

微量元素比值对研究中酸性侵入岩的物质来源具有重要意义(Taylor et al. , 1985),研究区花岗闪长岩和二长花岗岩的 Nb/Ta 值为 11.52~16.90,接近陆壳岩石(11±,Barbarin et al. , 1999),低于幔源岩石(17.5±);Zr/Hf 值 33.10~41.35,幔源岩石(36.27±2.00,Mcdonough and Sun, 1995),表明该岩浆的物质来源有幔源成分的参与;而辉石闪长岩

Rb/Sr 值为 0.09~0.14(陆壳 0.24),Zr/Hf 值 33.89~36.76(幔源岩石 36.27±2.00),进一步验证了岩浆形成早期下部地壳部分熔融过程中混入了幔源物质;综上所述,研究区中酸性侵入杂岩可能是俯冲板片流体交代的地幔楔,地幔楔部分熔融形成玄武质岩浆,玄武质岩浆底侵使得上覆地壳部分熔融的产物。

本文认为细粒辉石闪长岩⟶中粒花岗闪长岩⟶中细粒花岗闪长岩⟶中粒黑云母二长花岗岩岩浆可能是玄武质岩浆底侵而导致上覆年轻地壳的部分熔融的产物,其主要残留矿物相是石榴石和辉石等;从中粒花岗闪长岩⟶中细粒花岗闪长岩⟶中粒黑云母二长花岗岩浆演化过程发生了斜长石、黑云母、磷灰石等矿物相的分离结晶作用。

### 4.2　形成环境

北山地区位于西伯利亚板块、华北板块和塔里木板块交汇部位,研究区处北山造山带中段的明水—石板井—小黄山蛇绿岩带和红柳河—牛圈子—洗肠井蛇绿岩带之间,公婆泉—月牙山地体东部;经历了大陆基底的形成演化、大洋的俯冲—造山作用并伴随着大量的花岗岩形成、板内构造与盆地构造演化等三个大阶段,但晚古生代,尤其是晚古生代早期的构造环境还不是十分清楚(李舢等,2011)。研究区中泥盆世中酸性侵入杂岩整体呈岩基状产出,其岩石类型为 I 型花岗岩;在 Y—Nb 图解中落在火山弧和同碰撞花岗岩区内(图 10a),在(Y+Nb)—Rb 图解中落在火山弧花岗岩区内(图 10b),表明该杂岩具有火山弧花岗岩特征。小黄山蛇绿岩带中玄武岩和辉长岩的年龄分别为 336±4 Ma 和 345±14 Ma,且均具有大洋中脊的性质(Zheng Rongguo et al., 2013),表明小黄山洋还没有完全关闭,即晚泥盆世时期公婆泉岛弧带仍处于俯冲环境;同时研究区南侧,月牙山—洗肠井蛇绿岩中的玄武岩和辉长岩表现出弧后盆地火山岩的特征(郑国荣等,2012);而红柳河蛇绿岩带辉长岩堆晶的 SIMS 锆石 U-Pb 年龄为 516±7 Ma,之后被未变形的约 405 Ma 花岗岩侵入(郭召杰等,2006),表明月牙山—洗肠井蛇绿岩带所代表的弧后盆地在 405 Ma 之前已经闭合;此外研究区中酸性侵入杂岩呈现的洋壳岛弧或大陆边缘弧特征。因此由月牙山—洗肠井蛇绿岩代表的弧后盆地在石板井中酸性侵入杂岩侵位古生代地层之前已经闭合,为该区中酸性侵入杂岩的形成提供了陆源物质,其形成可能与小黄山洋向南俯冲有关;综上所述中泥盆世石板井中酸性侵入杂岩的形成于大洋岛弧背景下的火山弧环境,可能是小黄山洋向南俯冲的产物。

## 5　结论

通过对石板井地区中酸性侵入杂岩单颗粒锆石 U-Pb 定年、岩石元素的系统测定与分析,初步得出如下结论:

(1)细粒辉石闪长岩—中粒花岗闪长岩—中细

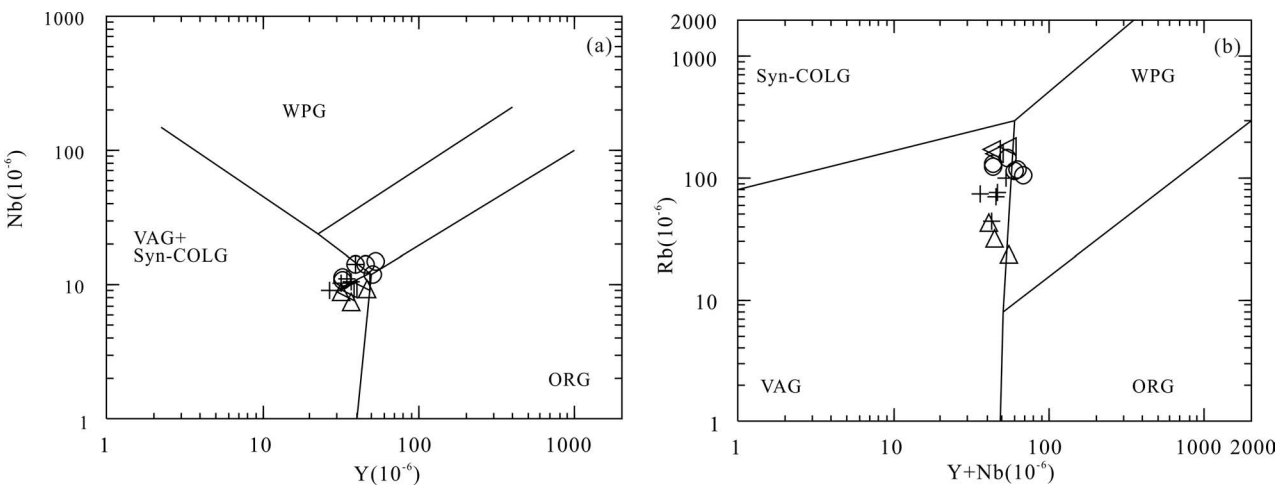


图 10 北山石板井地区花岗岩 Y—Nb 和 *R*1—*R*2 图解(据 Pearce et al.,1984,图例同图 8)

Fig. 10 Y—Nb and *R*1—*R*2 diagram for the granite (base map from Pearce et al.,1984) for the intrusive rocks in Shibanjing area, Beishan Mountains. The legend is the same as Figure 8)

Syn-COLG—碰撞同期花岗岩;VAG—火山弧花岗岩;WPG—板内花岗岩;ORG—洋脊花岗岩

Syn-COLG—collision granite; VAG—volcanic arc granite; WPG—in-plate granite; ORG—ocean granite

粒花岗闪长岩—中粒黑云母二长花岗岩形成时代为中泥盆世,年龄依次为 385.6±1.0 Ma、385.5±1.1 Ma、386.3±1.0 Ma、381.7±0.9 Ma。

(2)细粒辉石闪长岩—中粒花岗闪长岩—中细粒花岗闪长岩—中粒黑云母二长花岗岩具有 I 型花岗岩的特征;初始岩浆可能是俯冲板片流体交代的地幔楔,地幔楔部分熔融形成玄武质岩浆,玄武质岩浆底侵而导致上覆年轻地壳的部分熔融的产物,岩浆演化过程伴生以斜长石为主的矿物分离结晶作用。

(3)中泥盆世中酸性侵入杂岩的形成于大洋岛弧背景下的火山弧环境,可能是小黄山洋向南俯冲的产物。

**致谢**:由衷地感谢审稿专家和章雨旭研究员,他们为本文提供了宝贵的修改意见和建议,对文稿的改进和提升起到了重要作用!

## 参 考 文 献 / References

(The literature whose publishing year followed by a "&" is in Chinese with English abstract; The literature whose publishing year followed by a "#" is in Chinese without English abstract)

陈超,修迪,潘志龙,张欢,张金龙,李庆喆,专少鹏. 2017. 北山造山带中部早古生代伸展构造体制:来自石板井辉长岩的年代学及地球化学证据. 地质学报,91(8):1661~1673.

邓晋福,冯艳芳,狄永军,刘翠,肖庆辉,苏尚国,赵国春,孟斐,马帅,姚图. 2015b. 岩浆弧火成岩构造组合与洋陆转换. 地质论评,61(3):473~484.

邓晋福,刘翠,冯艳芳,肖庆辉,狄永军,苏尚国,赵国春,段培新,戴蒙. 2015a. 关于火成岩常用图解的正确使用:讨论与建议. 地质论评,61(4):717~734.

邓自华. 1965. 北山地区地质构造特征及其大地构造单元归属问题的初步讨论. 地质论评,23(3):172~180.

郭召杰,史宏宇,张志诚,张进江. 2006. 新疆甘肃交界红柳河蛇绿岩中伸展构造与古洋盆演化过程. 岩石学报,22(1):95~102.

侯可军,李延河,田有荣. 2009. LAMC-ICP-MS 锆石微区原位 U-Pb 定年技术. 矿床地质,28(4):481~492.

胡古月,李延河,范昌福,赵悦,侯可军,王天慧. 2015. 辽东古元古代菱镁矿矿床与硼酸盐矿床——同期异相沉积成矿探讨. 矿床地质,34(3):547~564.

江思宏,聂凤军,陈文,刘妍,白大明,刘新宇,张思红. 2003. 北山明水地区花岗岩时代的确定及其地质意义. 岩石矿物学杂志,22(2):107~111.

江思宏,聂凤军. 2006. 北山地区花岗岩类成因的 Nd 同位素制约. 地质学报,80(06):826~842.

李舢,王涛,童英,洪大卫,欧阳志侠. 2009. 北山柳园地区双峰山早泥盆世 A 型花岗岩的确定及其构造演化意义. 岩石矿物学杂志,28(5):407~422.

李舢,王涛,童英,王彦斌,洪大卫,欧阳志侠. 2011. 北山辉铜山泥盆纪钾长花岗岩锥石 U-Pb 年龄、成因及构造意义. 岩石学报,27(10):3055~3070.

刘雪亚,王荃. 1995. 中国西部北山造山带的大地构造及其演化. 地学研究,第 28 号:37~48.

刘雪亚. 1984. 甘肃北山区的钙碱系列岩浆活动及其与板块构造的关系. 地球学报,(3):157~171.

聂凤军,江思宏,白大明,刘妍,张义,赵月明,安存杰,王新亮,苏新旭. 2003. 蒙甘新相邻(北山)地区金铜矿床时空分布特征及成矿作用. 矿床地质, 22(3):234~245.

聂凤军,江思宏,白天明,等. 2002. 北山地区金属矿床成矿规律及找矿方向. 北京:地质出版社.

聂凤军,江思宏,赵省民,白大明. 2000. 北山北带古生代岩浆活动与金矿床的形成. 矿物岩石地球化学通报,19(4).

孙新春,张雨莲,高永伟. 2011. 甘蒙北山北带古生代地壳演化与成矿作用. 甘肃地质,(2):45~50.

王国强,李向民,徐学义,余吉远,过磊,闫巧娟,计波,武鹏. 2016. 甘蒙北山志留纪公婆泉群火山岩的地球化学及其对岩石成因和构造环境的制约. 地质学报,90(10):2603~2619.

王立社,杨建国,谢春林,雷永孝,王育习,曹红霞,杨鹏飞,齐亚林,金拴联. 2009. 甘肃北山火石山哈尔根头口布花岗岩年代学、地球化学及其地质意义. 地质学报,83(3):377~387.

许伟,徐学义,牛亚卓,宋博,陈高潮,史冀忠,张宇轩,李晨皓. 2019. 北山南部二叠纪海相玄武岩地球化学特征及其构造意义. 地质学报,93(8):1928~1953.

杨合群,李英,赵国斌,李文渊,王小红,姜寒冰,谭文娟,孙南一. 2010. 北山蛇绿岩特征及构造属性. 西北地质,43(1):26~36.

张文. 2013. 北山—阿拉善北缘晚古生代花岗岩及其构造意义. 导师:吴泰然. 北京:北京大学博士学位论文:1~201.

赵宏刚,梁积伟,王驹,苏锐,金远新,田霄,罗辉. 2019. 甘肃北山算井子埃达克质花岗岩年代学、地球化学特征及其构造意义. 地质学报,93(2):329~352.

赵振明,计文化,李文明. 2018. 北山南部玻基纯橄岩的发现及其岩石学和地球化学特征. 地质论评,64(5):1055~1077.

赵志雄,熊煜,贾元琴,王金荣,许海,高鉴,王新亮,刘强. 2018. 北山独龙包地区晚石炭世陆缘弧岩浆作用——花岗闪长岩锆石 U-Pb 年龄及地球化学证据. 地质论评, 64(03):79~91.

郑荣国,吴泰然,肖文交,张文,孟庆鹏. 2016. 北山北部双井子复式岩体年代学、地球化学及其大地构造意义. 地质学报,90(11):3153~3172.

郑荣国,吴泰然,张文,冯继成. 2012. 北山地区月牙山—洗肠井蛇绿岩的地球化学特征及形成环境. 地质学报,86(6):961~971.

左国朝,何国琦. 1990,北山板块构造及成矿规律. 北京:北京大学出版社: 1~209.

Barbarin B. 1999. A review of the relationships between granitoid types, their origins andtheir geodynamic environments. Lithos, 46(3):605~626.

Chappell B W, White A J R. 2001. Two contrasting granite types: 25 years later. Journal of the Geological Society of Australia, 48(4): 489~499.

Chen Chao, Xiu Di, Pan Zhilong, Zhang Huan, Zhang Jinlong, Li Qingzhe, Zhuan Shaopeng. 2017&. Early Paleozoic crustal extensional tectonic regime in the central part of Beishan Orogenic Belt: New evidence from geochronology and geochemistry of gabbro in Shibanjing. Acta Geologica Sinica, 91(8): 1661~1673.

Collins W, Beams S, White A, Chappell B W. 1982. Nature and origin of A-type granites with particular reference to southeastern Australia. Contributions to Mineralogy and Petrology, 80(2): 189~200.

Defant M J and Drummond M S. 1990. Derivation of some morden arc magmas by of young subducted lithosphere. Nature, 347: 662~665.

Deng Jinfu, Feng Yanfang, Di Yongjun, Liu Cui, Xiao Qinghui, Su Shangguo, Zhao Guochun, Meng Fei, Ma Shuai, Yao Tu. 2015b&. Magmatic arc and ocean—continent transition:

Discussion. Geological Review, 61(3): 473~484.

Deng Jinfu, Liu Cui, Feng Yanfang, Xiao Qinghui, Di Yongjun, Su Shangguo, Zhao Guochun, Dun Peixin, Duan Meng. 2015a&. On the correct application in the common igneous petrological diagrams: Discussion and suggestion. Geological Review, 61(4): 717~734.

Deng Zihua. 1965#. Preliminary discussion on the geological structure characteristics and the attribution of tectonic units in Beishan area. Geological Review, 23(3): 172~180.

Ding Jiaxin, Han Chunming, Xiao Wenjiao, Wang Zhongmei, Song Dongfang. 2017. Geochronology, geochemistry and Sr—Nd isotopes of the granitic rocks associated with tungsten deposits in Beishan district, NW China, Central Asian Orogenic Belt: Petrogenesis, metallogenic and tectonic implications. Ore Geology Reviews, 89: 441~462.

Guo Zhaojie, Shi Hongyu, Zhang Zhicheng, Zhang Jinjing. 2006&. The tectonic evolution of the south Tianshan paleo-oceanic crust inferred from the spreading structures and Ar-Ar dating of the Hongliuhe ophiolite, NW China. Acta Geologica Sinica, 22(1): 95~102.

Hou Kejun, Li Yanhe, Tian Yourong. 2009&. In situ U-Pb zircon dating using laser ablation-multi ion counting LA-ICP-MS. Mineral Deposits, 28(4): 481~492.

Hu Guyue, Li Yanhe, Fan Changfu, Zhao Yue, Hou Kejun, Wang Tianhui. 2015&. Paleoproterozoic magnesite and borate deposits from eastern Liaoning Province: with a discussion about synchrono-heteropic facies of sedimentary mineralization. Mineral Deposits, 34(3): 547~564.

Jahn B M, Windley B F, Natal'in B, Dobretsov N. 2004. Phanerozoic continental growth in Central Asia. Asian Earth Sci., 23: 599~603.

Jiang Sihong, Nie Feng, Chen Wen, Liu Yan, Bai Daming, Liu Xinyu, Zhang Sihong. 2003&. The determination of the emplacement age of granite in Mingshui, Beishan area, and its implication. Acta Petrologica et Mineralogica, 22(2): 107~111.

Jiang Sihong, Nie Feng. 2006&. Nd-isotope constraints on origin of granitoids in beishan mountain area. Acta Petrologica Sinica, 80(6): 826~842.

Jiang Sihong, Nie Fengjun, Liu Yan. 2004. Gold deposits in Beishan Mountain, northwestern China. Resource Geology, 325~340.

Jiang Sihong, Nie Fengjun. 2005. Geology and ore genesis of the Nanjinshan gold deposit in Beishan Mountain area, northwestern China. Biennial Sga Meeting.

Li Shan, Wilde Simon A, Wang Tao. 2013. Early Permian post-collisional high-K granitoids from Liuyuan area in southern Beishan orogen, NW China: Petrogenesis and tectonic implications. Lithos, 179: 99~119.

Li Shan, Wang Tao, TongYing, Hong Dawei, Ouyang Zhixia. 2009&. Identification of the Early Devonian Shuangfengshan A-type granites in Liuyuan area of Beishan and its implications to tectonic evolution. Acta Petrologica et Mineralogica, 28(5): 407~422.

Li Shan, Wang Tao, TongYing, Wang Yanbin, Hong Dawei, Ouyang Zhixia. 2011&. Zircon U-Pb age, origin and its tectonic significances of Huitongshan Devonian K-feldspar granites from Beishan orogen, NW China. Acta Geologica Sinica, 27(10): 3055~3070.

Liu Qian, Zhao Guochun, Sun Min, Eizenhoefer P, Han Yigui, Hou Wenzhu. 2015. Ages and tectonic implications of Neoproterozoic ortho- and paragneisses in the Beishan Orogenic Belt, China. Precambrian Research, 266: 551~578.

Liu Xueya, Wang Quan. 1995#. The geotectonic structure and evolution of the Beishan orogenic belt in western China. Proceedings of the Institute of Geology, (28): 37~48.

Liu Xueya. 1984&. Magmatism of calc-alkaline series in the beishan region of gansu province and its relation to plate tectonics. Acta Geosicientia Sinica, (3): 157~171.

Liu Yongsheng, Gao Shan, Hu Zhaochu, Gao Changgui, Zong Keqing, Wang Dongbing. 2010. Continental and oceanic crust recycling-induced melt—peridotite interactions in the Trans-North China Orogen: U-Pb dating, Hf isotopes and trace elements in zircons from mantle xenoliths. Journal of Petrology, 51(1~2): 537~571.

Liu Yongsheng, Hu Zhaochu, Gao Shan, Detlef Gunther, Xu Juan, Gao Changgui, Chen Haihong. 2008. In situ analysis of major and trace elements of anhydrous minerals by LA-ICP-MS without applying an internal standard. Chemical Geology, 257(1~2): 34~43.

Mcdonough W F, Sun S S. 1995. The composition of the Earth. Chemical Geology, 120(3~4)223~253.

Moynier, Frederic, Vance D, Fujii T, Savage P. 2017. The isotope geochemistry of zinc and copper. Reviews in Mineralogy and Geochemistry, 82(1):543~600.

Nie Fengjun, Jiang Sihong, Bai Daming, Liu Yan, Zhang Yi, Zhao Yueming, An Cunjie, Su Xinliang. 2003&. Temporal—spatial distribution and metallogenic processes of gold and copper deposits in Inner Mongolia—Gansu—Xinjiang border (Beishan) region. Mineral Deposits, 23(3): 234~245.

Nie Fengjun, Jiang Sihong, Bai Daming. 2002#. Metallogenic Regularity and Prospecting Direction of Metal Deposits in Beishan Area. Beijing: Geological Publishing House.

Nie Fengjun, Jiang Sihong, Zhao Shengmin, Bai Daming. 2000#. Paleozoic magmatic activity and the formation of gold deposits in Beishan North Belt. Bullet in of Mineralogy, Petrology and Geochemisty, 19(4).

Pitcher W S. 1983. Granite type and tectonic environment. In: Hsu K J. ed. Mountain Building Processes. London: Academic Press: 19~40.

Song Dongfang, Xiao Wenjiao, Han Chunming, Tian Zhonghua, Wang Zhongmei. 2013. Provenance of metasedimentary rocks from the Beishan orogenic collage, southern Altaids: constraints from detrital zircon U-Pb and Hf isotopic data. Gondwana Res. 24, 1127~1151.

Song Dongfang, Xiao Wenjiao, Han Chunming, Tian Zhonghua. 2014. Geochronological and geochemical study of gneiss—schist complexes and associated granitoids, Beishan Orogen, southern Altaids. International Geology Review. 55, 1705~1727.

Song Dongfang, Xiao Wenjiao, Windley B F, Han C, Tian Z. 2015. A Paleozoic Japan-type subduction—accretion system in the Beishan orogenic collage, southern Central Asian Orogenic Belt. Lithos, 224~225: 195~213.

Su Benxun, Qin Kezhang, Sakyi P A, Tang Dongmei, Liu Pingping, Malaviarachchi S P K. 2012. Geochronologic—petrochemical studies of the Hongshishan mafic - ultramafic intrusion, Beishan area, Xinjiang (NW China): petrogenesis and tectonic implications. International Geology Review, 54(3): 270~289.

Sun Xinchun, Zhang Yulian, Gao Yongwei. 2011&. Paleozoic crustal evolution and mineralization of the northern Baishan in Gansu. Gansu Geology, (2): 45~50.

Taylor S R, McLennan S M. 1985. The continental crust: Its composition and evolution. Blackwell Scientific: 1~312.

Wang Guoqiang, Li Xiangmin, Xu Xueyi, Yu Jiyuan, Guo Lei, Yan Qiaojuan, Ji Bo, Wu Peng. 2016&. Geochemistry of Gongpoquan group in the Beishan area, Gansu Province: Constraints on petrogenesis and tectonic setting. Acta Geologica Sinica, 90(10): 2603~2619.

Wang Lishe, Yang Jianguo, Xie Chunlin, Lei Yongxiao, Wang Yuxi, Cao Hongxia, Yang Pengfei, Qi Yalin, Jin Shuanlian. 2009&. Geochronology and geochemistry of Haergentoukoubu granites in the Beishan area, Gansu, China and their geological significance. Acta Geologica Sinica, 83(3):377~387.

Wang Xinyu, Yuan Chao, Zhang Yunying, Long Xiaoping, Sun Min, Wang Lixing, Soldner J, Lin Zhengfan. 2018. S-type granite from the Gongpoquan arc in the Beishan Orogenic Collage, southern Altaids: Implications for the tectonic transition. Journal of Asian Earth Sciences, 153: 206~222.

Xiao Wenjiao, Mao Qigui, Windley B F, Han Chunming, Qu Junfeng, Zhang Jien, Ao Songjian, Guo Qianqian, Cleven N R, Lin S F, Shan Y H, Li J L. 2010. Paleozoic multiple accretionary and collisional processes of the Beishan orogenic collage. Am. J. Sci., 310: 1553~1594.

Xu Wei, Xu Xueyi, Niu Yazhuo, Song Bo, Chen Gaochao, Shi Jizhong, Zhang Yuxuan, Li Chenhao. 2019&. Geochronology and petrogenesis of the Permian marine basalt in the southern Beishan region and their tectonic implications. Acta Geologica Sinica, 93(8): 1928~1953.

Yang Hequn, Li Ying, Zhao Guobin, Li Wenyuan, Wang Xiaohong, Jiang Hanbing, Tan Wenjuan, Sun Nanyi. 2010&. Characteristics and geotectonic significance of the ophiolites in Beishan area. Northwestern Geology, 43(1): 26~36.

Zhang Wen. 2013&. Late Paleozoic Granitoids in Beishan—Northern Alxa Area and Their Tectonic Implications. Tutor: Wu Tairan. Beijing: Ph. D. thesis of Peking University:1~201.

Zhao Honggang, Liang Jiwei, Wang Ju, Su Rui, Jin Yuanxin, Tian Xiao, Luo Hui. 2019&. Geochronology and geochemical characteristics of the Suanjingzi adakitic granites in the Beishan Mountains, Gansu Province, China, and their tectonic significance. Acta Geologica Sinica, 93(2): 329~352.

Zhao Keqiang, Sun Jinggui, Bai Lingan, Zhang Yong, Gu Alei. 2017. Petrogenesis and Mo mineralization of a granitic complex, Da Hinggan Mountains, NE China: insights from zircon U-Pb dating, major and trace element geochemistry, and Sr—Nd—Pb isotopes. Geological Journal, 52: 110~130.

Zhao Zhenming, Ji Wenhua, Li Wenming. 2018&. Discovery of vitric dunite (meimechite) in southern Beishan Mountain, and its petrological and geochemical characteristics. Geological Review, 64(5): 1055~1077.

Zhao Zhixiong, Xiong Yu, Jia Yuanqin, Wang Jinrong, Xu Hai, Gao Jian, Wang Xinliang, Liu Qiang. 2018&. The continental arcs magmatic at the Dulongbao Area in Beishan orogenic belt in Late Carboniferous: evidences from zircon U-Pb dating and geochemistry of the granodiorite. Geological Review, 64(3): 597~609.

Zheng Rongguo, Wu Tairan, Wen Zhang, Xu Cao, Meng Qingpeng. 2013. Late Paleozoic subduction system in the southern Central Asian Orogenic Belt: Evidences from geochronology and geochemistry of the Xiaohuangshan ophiolite in the Beishan orogenic belt. Journal of Asian Earth Sciences, 62: 463~475.

Zheng Rongguo, Wu Tairan, Xiao Wenjiao, Zhang Wen, Meng Qingpeng. 2016&. Geochronology, geochemistry and tectonic implications of the Shuangjizi composite pluton in the Northern Beishan. Acta Geologica Sinica, 90(11): 3153~3172.

Zheng Rongguo, Wu Tairan, Zhang Wen, Feng Jicheng. 2012&. Geochemical characteristics and tectonic setting and of the Yueyashan—Xichangjing ophiolite in the Beishan Area. Acta Geologica Sinica, 86(6): 961~971.

Zuo Guochao, He Guoqi. 1990#. Tectonics and Metallogenic Regularity of the Beishan Plate. Beijing: Peking University Press: 1~209.

# The LA-ICP-MS Zircon U-Pb ages and geochemical characteristics of Late Paleozoic intermediate—acidic intrusive complexes in Shibanjing area, Beishan Mountains, Inner Mongolia, and their geological significance

ZHAO Keqiang, MA Shengming, XI Mingjie, YANG Jianzhou, CAI Yongwen, GONG Jingjing

*Institute of Geophysical and Geochemical Exploration, Chinese Academy of Geological Science, Langfang, Hebei*, 065000

**Objectives**: The magmatic source, forming environment and tectonic setting were revealed by the age and geochemical characteristics of granite. Recently, during the geological survey and related scientific research work in the Shibanjing area of Inner Mongolia, we identified a set of Middle Devonian intermediate—acidic intrusive complexes in the Shibanjing area. In this study, we discuss the petrogenesis, forming environment and tectonic setting of intemediate—acidic intrusive complexes.

**Methods**: Based on field work, through the microscope, zircon U-Pb dating, whole-rock major and trace element geochemistry were carried out.

**Results**: The results show that the fine-grained augite diorite, medium-grained granodiorite, medium to fine-grained granodiorite and medium-grained biotite monzogranite formed in the Middle Devonian(385~380 Ma), and they have homologous magma evolution characteristics. The fine-grained pyroxenite diorite belongs to the calc-alkaline, sodic, peraluminous series. The medium -grained granodiorite, medium to fine-grained granodiorite and

medium-grained biotite monzogranite characterized by the high-K calc-alkaline to calc-alkaline, sodic, metaluminous—peraluminous series.

**Conclusions**: The parent magma has been considered to be connected with the mantle wedge was metasomatized by the subducted plate fluid, and the partial melting of the mantle wedge forms basalt magma. The basalt magma underplating during the partial melting of lower crust. In the process, it is accompanied by the crystallization and differentiation of magma. The Middle Devonian intermediate—acidic intrusive complexes have the characteristics of type I granite, and it is volcanic arc environment formed in the background of the Oceanic island arc, the diagenetic environment may belongs to the southward subduction under the background of the Xiaohuangshan Ocean.

**Keywords**: intemediate—acidic intrusive complexes; element geochemistry; Middle Devonian; zircon U-Pb dating; Shibanjing area, Beishan Mountains, Inner Mongolia

**Acknowledgements**: This work was sponsored by Public Geological Survey project of China Geological Survey (Nos. DD20160040, DD20190570 and DD20190571).

**First author**: ZHAO Keqiang, male, born in 1986, Doctor of Philosophy Degree. Mainly engaged in Mineralogy, Petrology, Economic Geology. Address: No. 84, Jinguangdao Street, Guangyang District, Langfang, Hebei, 065000. Email: zhaokeqiang@ igge. cn

Manuscript received on: 2019-04-14; Accepted on: 2019-08-18; Edited by: ZHANG Yuxu

**Doi**: 10. 16509/j. georeview. 2020. 01. 005